

WATER SOLUBLE POLYMER STABILIZED IRON(0) NANOCCLUSERS: A
COST EFFECTIVE AND MAGNETICALLY RECOVERABLE CATALYST IN
HYDROGEN GENERATION FROM THE HYDROLYSIS OF AMMONIA
BORANE

A THESIS SUBMITTED TO
THE GRADUATE SCHOOL OF NATURAL AND APPLIED SCIENCES
OF
MIDDLE EAST TECHNICAL UNIVERSITY

BY

MELEK DİNÇ

IN PARTIAL FULFILLMENT OF THE REQUIREMENT
FOR
THE DEGREE OF MASTER OF SCIENCE
IN
CHEMISTRY

JULY 2011

Approval of the thesis:

**WATER SOLUBLE POLYMER STABILIZED IRON(0) NANOCCLUSERS:
A COST EFFECTIVE AND MAGNETICALLY RECOVERABLE
CATALYST IN HYDROGEN GENERATION FROM THE HYDROLYSIS OF
AMMONIA BORANE**

Submitted by **MELEK DİNÇ** in partial fulfillment of the requirements for the degree of **Master of Science in Chemistry Department, Middle East Technical University** by,

Prof. Dr. Canan Özgen
Dean, Graduate School of **Natural and Applied Sciences**

Prof. Dr. İlker Özkan
Head of Department, **Chemistry**

Prof. Dr. Saim Özkâr
Supervisor, **Chemistry Dept., METU**

Examining Committee Members:

Prof. Dr. Gülsün GÖKAĞAÇ
Chemistry Dept., METU

Prof. Dr. Saim ÖZKAR
Chemistry Dept., METU

Prof. Dr. Ceyhan KAYRAN
Chemistry Dept., METU

Assoc. Prof. Dr. Ayşen YILMAZ
Chemistry Dept., METU

Prof. Dr. İnci Eroğlu
Chemical Engineering Dept., METU

Date: 06/07/2011

I hereby declare that all information in this document has been obtained and presented in accordance with academic rules and ethical conduct. I also declare that, as required by these rules and conduct, I have fully cited and referenced all material and results that are not original to this work.

Name, Last name: Melek DİNÇ

Signature :

ABSTRACT

WATER SOLUBLE POLYMER STABILIZED IRON(0) NANOCCLUSERS: A COST EFFECTIVE AND MAGNETICALLY RECOVERABLE CATALYST IN HYDROGEN GENERATION FROM THE HYDROLYSIS OF AMMONIA BORANE

Dinç, Melek

M.Sc., Department of Chemistry

Supervisor: Prof. Dr. Saim Özkar

July 2011, 65 pages

The property transition metal nanoclusters are more active catalysts than their bulk counterparts because of increasing proportion of surface atoms with decreasing particle size. The development of efficient and economical catalysts to further improve the kinetic properties under moderate conditions is therefore important for the practical application of nanoclusters as catalyst in the hydrogen generation from hydrolysis of ammonia borane. In this regard, the development of active iron catalysts is a desired goal because it is the most ubiquitous of the transition metals, the fourth most plentiful element in the Earth's crust. In this dissertation, we report the preparation, characterization and investigation of the catalytic activity of the water soluble polymer stabilized iron(0) nanoclusters. They were prepared from the reduction of iron(III) chloride by a mixture of sodium borohydride (NaBH₄, SB) and ammonia borane (H₃NBH₃, AB) mixture in the presence of polyethylene glycol (PEG) as stabilizer and ethylene glycol as solvent at 80 °C under nitrogen atmosphere. PEG stabilized iron(0) nanoclusters were isolated from the reaction solution by centrifugation and characterized by SEM, EDX, TEM, HRTEM, XRD, UV-Vis, ICP-OES and FT-IR techniques. PEG stabilized iron(0) nanoclusters have almost uniform size distribution with an average particle size of 6.3 ± 1.5 nm. They

were redispersible in water and yet highly active catalyst in hydrogen generation from the hydrolysis of AB. They provide a turnover frequency of TOF = 6.5 min^{-1} for the hydrolysis of AB at $25.0 \pm 0.5 \text{ }^\circ\text{C}$. The TOF value is the best ever reported among the Fe catalyst and comparable to other non-noble metal catalyst systems for the catalytic hydrolysis of AB. Kinetics of hydrogen generation from the hydrolysis of AB in the presence of PEG stabilized iron(0) nanoclusters were also studied by varying the catalyst concentration, substrate concentration, and temperature. This is the first kinetic study on the hydrolysis of AB in the presence of an iron catalyst. Moreover, PEG stabilized iron(0) nanoclusters can be separated magnetically from the catalytic reaction solution by using a magnet and show catalytic activity even after tenth run.

Keywords: Iron nanoclusters, Polyethylene glycol, Catalyst, Sodium Borohydride, Hydrolysis of Ammonia Borane.

ÖZ

SUDA ÇÖZÜNÜR POLİMERLE KARARLILAŞTIRILMIŞ DEMİR(0) NANOKÜMELERİ: HAZIRLANMASI, TANIMLANMASI VE AMONYAK BORANIN HİDROLİZİNDE KATALİTİK ETKİNLİĞİ

Dinç, Melek

Yüksek Lisans, Kimya Bölümü

Tez Yöneticisi: Prof. Dr. Saim Özkâr

Temmuz 2011, 65 sayfa

Geçiş metal nanokümelерinin, parçacık boyutları küçüldükçe yüzey alanları büyümektedir ve bu özelliklerinden ötürü geçiş metal nanokümeleri, külçe metallere nazaran daha aktif katalizörlerdir. Pahalı metallerin pratik uygulamalarda katalizör olarak kullanımındaki kaygılar nedeniyle; istenilen koşullarda amonyak boranın hidrolizinden hidrojen salıverilmesi için, etkin ve daha ucuz metal katalizörlerin geliştirilmesi amaçlanmaktadır. Bu bağlamda; yer kabuğunda bulunma yüzdesi bakımından dördüncü sırada yer alan demirin nanokümelерinin hazırlanarak, amonyak boranın hidrolizinde etkin bir katalizör olarak geliştirilmesi amaçlanmaktadır. Katalizör olarak kullanılacak demir(0) nanokümeleri, demir(III) klorürün etilen glikol içerisinde suda çözünür bir polimer olan polietilen glikol (PEG) varlığında 80 °C’de indirgenmesi sonucunda hazırlandı. Polimer ile kararlılaştırılmış demir(0) nanokümeleri santrifüjlemeyle izole edildikten sonra SEM, EDX, TEM, HR-TEM, XRD, UV-görünür ve FT-IR teknikleri kullanılarak tanımlandı. Hazırlanan ve tanımlanan suda çözünür polimerle kararlılaştırılmış demir(0) nanokümeleri, amonyak boranın hidrolizinde katalizör olarak sınıandı. Polimerle kararlılaştırılmış demir(0) nanokümeleri, ortalama 6.3 ± 1.5 nm parçacık boyutuyla homojen bir dağılıma sahiptir. Su içerisinde kolayca dağılabilen, PEG ile kararlılaştırılmış demir(0) nanokümeleri; amonyak boranın hidroliziyle hidrojen

eldesinde oldukça etkin katalizörlerdir. Deneysel sonuçlar, PEG ile kararlaştırılmış demir(0) nanokümlerinin oda sıcaklığında, düşük katalizör ve tepken derişimlerinde bile amonyak boranın hidrolizinde etkin olduğunu gösterdi. PEG ile kararlaştırılmış demir(0) nanokümleri, $25.0 \pm 0.5 \text{ }^\circ\text{C}$ ' de sağlamış olduğu 6.5 dk^{-1} gibi bir çevrim frekansı ile amonyak boranın hidrolizinde bugüne kadar bilinen demir katalizörleri arasında en yüksek etkinliği göstermektedir. Katalitik hidroliz tepkimesinin kinetiği, katalizör derişimine, tepken derişimine ve sıcaklığa bağılı olarak ayrıntılı bir şekilde incelendi. Elde edilen kinetik veriler kullanılarak, amonyak boranın katalitik hidrolizinin aktivasyon parametreleri hesaplandı. Bu çalışma demir katalizörünün AB hidrolizinde kullanılmasıyla ilgili yapılan ilk kinetik çalışmadır. Buna ek olarak, PEG ile kararlaştırılmış demir(0) nanokümleri manyetik olarak tepkime ortamından mıknatıs yardımıyla ayrılabilir ve onuncu çevrim sonunda bile katalitik etkinlik göstermektedirler.

Anahtar kelimeler: Demir nanokümleri, Polietilen Glikol, Katalizör, Sodyum Borhidrür, Amonyak Boranın Hidrolizi.

To my parents,

ACKNOWLEDGEMENT

I have been indebted in the preparation of this thesis to my supervisor, Prof. Dr. Saim Özkar whose patience and kindness, as well as his academic experience, have been invaluable to me. I appreciate all his contributions of time, ideas, and funding to make my experience productive and stimulating.

I am also grateful to the Assist. Prof. Dr. Önder Metin for his endless help. Throughout all of the master period, he provided encouragement, sound advice, good teaching, good company, and lots of good ideas and I would have been lost without him.

I also would like to express my thanks to my labmates Serdar Akbayrak, Salim Çalışkan, Derya Çelik, Huriye Erdoğan, Murat Rakap, Ebru Ünel, Selin Şencanlı, Dr. Mehmet Zahmakıran, Dr. Mehdi Masjedi, Dr. Senem Karahan, Assist. Prof. Dr. Sibel Duman, , Assoc. Prof. Dr. Yalçın Tonbul for their motivation and friendship during my studies.

I especially thank to Tuğçe Ayvalı for being my best friend who always being there whenever I need and also my siblings Çiğdem Dinç, Ayberk Dinç, Hilal Çetin and my brother in law Veysel Çetin for their love, patience, moral support and encouragement in every moment of my life.

I would like to thanks to TUBITAK for Grant TBAG-108T840.

Lastly, and most importantly, I wish to thank my parents, Fidan Dinç and Yusuf Dinç. They bore me, raised me, always supported me, taught me, and loved me who made everything possible for me unconditionally. To them I dedicate this thesis.

TABLE OF CONTENTS

ABSTRACT.....	iv
ÖZ.....	vi
ACKNOWLEDGEMENT.....	ix
TABLE OF CONTENTS.....	x
LIST OF FIGURES.....	xii
LIST OF TABLES.....	xv
LIST OF ABBREVIATIONS.....	xvi
CHAPTERS.....	1
1. INTRODUCTION.....	1
2. HYDROGEN ECONOMY.....	4
2.1. Hydrogen as an Energy Carrier.....	4
2.2. The Storage Challenge of Hydrogen.....	5
3. TRANSITION METAL(0) NANOCCLUSERS AS CATALYST.....	9
3.1. Transition Metal(0) Nanoclusters.....	9
3.2. Stabilization of Transition Metal(0) Nanoclusters.....	11
3.2.1. Electrostatic Stabilization (DLVO Theory).....	12
3.2.2. Steric Stabilization.....	13
3.2.3. Electrosteric Stabilization.....	15
3.3. Synthesis of Transition Metal(0) Nanoclusters.....	16
3.4. Transition Metal(0) Nanoclusters in Catalysis.....	17
3.4.1. General Concepts of Catalysis.....	17
3.4.2. Definitions of Catalytic Terms.....	20

3.4.3. The Characterization Methods of Transition Metal Nanoclusters.....	20
3.4.4. Surface Area Effect of Heterogeneous Catalysis in Catalytic Activity	22
4. EXPERIMENTAL	24
4.1. Materials	24
4.2. Preparation of PEG Stabilized Iron(0) Nanoclusters.....	24
4.3. Characterization of PEG Stabilized Iron(0) Nanoclusters.....	26
4.4. Testing the Catalytic Activity of PEG Stabilized Iron(0) Nanoclusters in the Hydrolysis of AB.....	27
4.5. Quantification of the Liberated NH ₃ Gas	28
4.6. Effect of PEG Concentration on The Catalytic Activity of Iron(0) Nanoclusters in The Hydrolysis of AB	29
4.7. Kinetics of Hydrolysis of AB Catalyzed by PEG Stabilized Iron(0) Nanoclusters	29
4.8. Catalytic Lifetime of PEG Stabilized Iron(0) Nanoclusters in the Hydrolysis of AB	30
4.9. Reusability of PEG Stabilized Iron(0) Catalyst in The Hydrolysis of AB.....	30
5. RESULTS AND DISCUSSION	31
5.1. Preparation and Characterization of PEG Stabilized Iron(0) Nanoclusters	31
5.2. Catalytic Activity and Kinetics of Hydrolysis of AB Catalyzed by PEG Stabilized Iron(0) Nanoclusters.....	40
80EQPENWUQP (.....):	
REFERENCES.....	(iii)..... 50
APPENDICES	(iii)..... 62

LIST OF FIGURES

FIGURES

Figure 1. Comparison of gravimetric and volumetric densities of various hydrogen storage materials.....	7
Figure 2. Melting point behavior of gold nanoparticles.....	10
Figure 3. The comparison of the electronic states in (a) a bulk metal particle (b) a large cluster of cubic close packed atoms, (c) simple triatomic cluster	11
Figure 4. Schematized aggregation of nanoparticles in the presence and absence of stabilizing agents.....	12
Figure 5. Plot of the energy versus interparticular distance for electrostatic stabilization and the schematic representation of the electrostatic stabilization of transition metal nanoclusters.....	12
Figure 6. The schematic illustration of steric stabilization of the metal nanoclusters.	13
Figure 7. Structure model of polymer-stabilized metal nanoclusters.....	14
Figure 8. Two models suggested for the stabilization of the metal nanocluster by a polymer; (a) the stabilization of each nanocluster by one polymer chain (the widely accepted one); (b) the stabilization of many nanoclusters by one polymer chain.	15
Figure 9. Schematics of electrosteric stabilization: (a) charged particles with nonionic polymers; (b) polyelectrolytes attached to uncharged particles.....	16
Figure 10. The classification of catalysts	18
Figure 11. Schematic representation of the energetics in catalytic cycle.....	19
Figure 12. The common methods of characterization of transition metal nanoclusters.....	22

Figure 13. Idealized representation of hexagonal close-packed full-shell ‘magic number’ clusters and the relation between the total number of atoms in full shell clusters and the percentage of surface atoms	23
Figure 14. The experimental setup used for the preparation of PEG stabilized iron(0) nanoclusters.....	25
Figure 15. The experimental setup used in performing the catalytic hydrolysis of ammonia borane and measuring the hydrogen generation rate.....	28
Figure 16. UV-Visible electronic absorption spectra of iron(III) chloride in the presence of PEG before and after injection of sodium borohydride and AB mixture.	32
Figure 17. a) SEM image and b) corresponding electron mapping for Fe atoms of PEG stabilized iron(0) nanoclusters.....	33
Figure 18. SEM-associated EDX spectrum of the PEG stabilized iron(0) nanoclusters.....	34
Figure 19 a) Low resolution TEM image b) corresponding particle size histogram of PEG stabilized iron(0) nanoclusters.....	35
Figure 20. HRTEM image of the PEG stabilized iron(0) nanoclusters taken from the methanol solution	36
Figure 21. X-ray diffraction patterns of PEG stabilized iron(0) nanoclusters prepared from the reduction of iron(III) chloride by a) sodium borohydride and b) a mixture of sodium borohydride and ammonia borane.....	37
Figure 22. (a) The plot of volume of hydrogen generated versus time during the hydrolysis of AB catalyzed by PEG stabilized Fe(0) nanoclusters at different PEG to Fe ratio and TEM images of PEG stabilized Fe(0) nanoclusters at different [PEG]/[Fe] ratios, (b) [PEG]/[Fe]= 2, (c) [PEG]/[Fe]= 3, (d) [PEG]/[Fe]= 4.	39
Figure 23. IR spectra of the PEG stabilized iron(0) nanoclusters and neat PEG, both taken by using ATR cell.....	40

Figure 24. a) The volume of hydrogen versus time plots depending on metal concentration for PEG-stabilized iron(0) nanoclusters at 25.0 ± 0.5 °C. b) The plot of hydrogen generation rate versus the concentration of metal (both in logarithmic scale). 41

Figure 25. a) The volume of hydrogen versus time plots depending on the substrate concentrations at constant catalyst concentration for the hydrolysis of AB catalyzed by PEG stabilized Fe(0) nanoclusters (25.0 mM Fe) at 25.0 ± 0.5 °C. b) The plot of hydrogen generation rate versus the concentration of the substrate (both in logarithmic scale). 43

Figure 26. a) The volume of hydrogen versus time plots at different temperatures for the hydrolysis of AB (200.0 mM) catalyzed by PEG-stabilized iron(0) nanoclusters (25.0 mM) in the temperature range 15.0-35.0 °C. b) The Arrhenius plot ($\ln k$ versus the reciprocal absolute temperature $1/T$ (K^{-1})). 45

Figure 27. a) Volume of hydrogen versus time plots for the hydrolysis of AB catalyzed by PEG stabilized iron(0) nanoclusters during the reusability test. b) A photograph representing the magnetically recovery of PEG stabilized iron(0) nanoclusters after each catalytic run. 47

LIST OF TABLES

TABLES

Table 1.	44
Table A.1. Volume of hydrogen generated versus time for the hydrolysis of ammonia borane catalyzed by PEG stabilized iron(0) nanoclusters in different polymer concentrations.	82
Table A.2. Volume of hydrogen generated versus time for the hydrolysis of ammonia borane catalyzed by PEG stabilized iron(0) nanoclusters in different iron(III) chloride concentrations in the range of 5-25 mM.	83
Table A.3. Volume of hydrogen generated versus time for the hydrolysis of ammonia borane catalyzed by PEG stabilized iron(0) nanoclusters in different H ₃ NBH ₃ concentrations in the range of 100-1500 mM.	84
Table A.4. Volume of hydrogen generated versus time for the hydrolysis of ammonia borane catalyzed by PEG stabilized iron(0) nanoclusters at different temperatures in the range of 15-35 °C.....	85

LIST OF ABBREVIATIONS

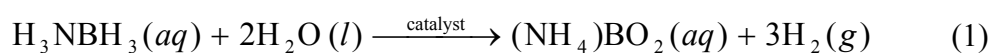
NPs	: Nanoparticles
NCs	: Nanoclusters
PEG	: Polyethylene Glycol
AB	: Ammonia Borane
E_a^{apparent}	: Apparent Activation Energy
TOF	: Turnover Frequency
TTON	: Total Turnover Number
V	: Rate of Reaction
ΔG	: Change in Gibbs Free Energy
ΔH^\ddagger	: Enthalpy of Activation
ΔS^\ddagger	: Entropy of Activation
J	: Coupling Constant
k_{app}	: Apparent Rate Constant
Ppm	: Parts per Million

CHAPTER 1

INTRODUCTION

Natural processes led to spontaneous accumulation of carbon based energy sources so called fossil fuels which have been used to produce around 80% of the world energy demand [1]. However, the fact that reserves of the fossil fuels are depletable and that the combustion of them accounts for the climate change due to the greenhouse gases released into atmosphere [2]. In this regard, the renewable energy sources have been extensively studied as an alternative source to fossil fuels. However, not only the problem of their discontinuity but also the on-going major problems such as low efficiency and high cost in the use of renewable energy sources needs to storage of energy. In this manner, hydrogen seems to be the best energy carrier because it is a secure and abundant, clean, renewable source and widely available from different domestic sources [3]. Many efforts have been devoted to use hydrogen as an energy carrier in our daily life applications for a decade and many successful systems have been developed in recent years [4,5]. The main problem is to store hydrogen in large quantities without taking up a significant amount of space in a safe way [6]. In this regard, developing safe, reliable, compact, and cost-effective hydrogen storage technologies is essential for the widespread usage of hydrogen as a energy form [6]. Chemical hydrides, especially boron hydrides, have been tested for solid state hydrogen storage materials because of their relatively high gravimetric hydrogen density and low molecular weights [7,8]. Among boron hydrides, ammonia

borane (H_3NBH_3 , AB) has recently been attracting a great deal of attention as a hydrogen storage material due to its high hydrogen content (19.6 wt %)[9,10], stability and safety under fuel cell operating conditions [11]. AB releases hydrogen upon hydrolysis according to Eq.(1) only in the presence of suitable catalysts [12,13].



Many catalyst systems including transition metals and their alloys have been tested for hydrogen generation from the hydrolysis of AB [14], but the fast hydrogen generation was achieved only in the presence of noble metal catalysts such as Pt, Rh and Ru at room temperature [15,16]. Due to the concerns over the practical use of such expensive metals as catalyst, the development of an effective and low-cost non-noble metal catalyst system to further improve the kinetic properties under moderate conditions is essential for the practical application of this system. In this regard, despite of several nickel and cobalt catalysts have been reported in the hydrolysis of AB [17,18,19,20,21,22,23], to best our knowledge, there is only one study on the use of iron catalyst in the hydrolysis of AB [24], reporting that the amorphous iron nanoparticles generated in situ from the reduction of iron(II) sulfate by SB-AB mixture are active catalyst providing a turnover frequency of 3.1 min^{-1} in the hydrolysis of AB. Considering the fact that iron is the most ubiquitous of the transition metals, the development of more active and stable iron catalyst for the hydrolysis of AB is desired. One promising way of increasing activity is the use of transition metals in the form of nanoclusters as catalyst because a large percentage of atoms lies on the surface of nanoclusters [25,26]. However, the high reactivity of nanoclusters and lack of neighbouring atoms cause the tendency toward the aggregation resulted with deterioration of basic magnetic properties of iron. This aggregation between nanoclusters make stabilization a major need in production of materials based on magnetic metal nanoclusters [27]. The large unit number of polymers extensively are used as the medium for steric stabilization of magnetic nanoclusters and also large polymers can be used as a stabilizer with long chains and

they surrounded to the surface of metal nanoclusters by extending out their long chains. This steric barrier supply important advantage for liquid phase catalytic applications [28]. The simplest and frequently cited explanation involves adsorption of a great number of polymer chain fragments at a metal particle, when summation of numerous separate weak dispersion interactions gives a considerable energy gain upon such stabilization. It is also believed that polymer chains block the free valences of surface atoms, thus creating a steric barrier to further growth of nanoparticles [29]. In addition, polyols were used as an alternatives for water as coordinating solvents because of relatively high dielectric constant and high donor number which form better interactions with metal ions [27]. For instance, ethylene glycol occupies a special place for magnetic nanoclusters and it is good solvent for iron.

Herein, we report the synthesis and characterization of water soluble polymer stabilized iron(0) nanoclusters catalyst and its use in hydrogen generation from the hydrolysis of AB. Polymer stabilized iron(0) nanoclusters were prepared from the reduction of iron(III) chloride by a mixture of SB and AB in the presence of polyethylene glycol (PEG) in ethylene glycol (EG) solution at 80 °C. They are stable enough in solution to be isolated as solid material by centrifugation and characterized by SEM, EDX, TEM, XRD, ATR-IR, ICP-OES and UV-visible electronic absorption spectroscopy. PEG stabilized iron(0) nanoclusters are redispersible in water and yet show high catalytic activity in the hydrolysis of AB. The hydrolysis of AB catalyzed by PEG stabilized iron(0) nanoclusters was followed by monitoring the volume of hydrogen generation versus time. Kinetics of catalytic hydrolysis of AB was studied depending on the catalyst concentration, substrate concentration, and temperature. This is the first kinetic study on the hydrolysis of AB in the presence of an iron catalyst. Moreover, PEG stabilized iron(0) nanoclusters can be recovered from the catalytic solution by using a magnet and reused in the hydrolysis of AB at 25.0 ± 0.5 °C.

CHAPTER 2

HYDROGEN ECONOMY

2.1. Hydrogen as an Energy Carrier

According to the International Energy Agency (IEA) [30], energy production from known oil and gas resources will fall by around 40-60 per cent by 2030. If everyone in the world used oil at the same rate, the world's proven oil reserves would be used up in less than 10 years [31]. Competition for fossil fuel resources is a source of international tension, and potentially conflict. Even if fossil fuel resources were depletable, we would have another compelling reason for an urgent switch to renewable energy: climate change because of global warming threatens the fragile balance of our planet's ecosystems and could consign a quarter of all species to extinction [32]. Using renewable energy sources such as wind power, solar and geothermal energy, biomass, biofuels and photovoltaic energy incontestably causes to dramatic climate change. However, some of these renewable sources have discontinuity problem and also construction of plants is relatively expensive. Regarding these problems, hydrogen seems to be the best solution of the present energy problems.

Hydrogen is an energy carrier which is meaning it can be stored and delivered energy in an considerably operable form. Even though hydrogen is one of the most plentiful element on Earth, it combines readily with other elements and is always

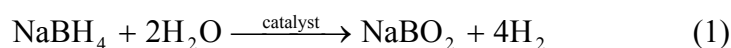
found as a part of other compound, such as water or hydrocarbons like natural gas (which consists mainly of methane). Hydrogen is also found in biomass which contains all plants and animals [33].

Hydrogen can be produced using a variety of resources including biomass, hydro, wind, solar, geothermal, nuclear, coal with carbon sequestration, and natural gas. This great potential for diversity of sources makes hydrogen a promising energy carrier [34]. The issues on hydrogen production, storage and transmission, as well as the use of hydrogen notably as fuel for fuel cells have been studied on the title of ‘Hydrogen Economy’. The current work is that fuel cells will experience a significant price reduction along with the development of the fields of application and that infra-structure problems will eventually be solved. Production of hydrogen fuel is more expensive than that of the fuels already in use, yet is expected to decrease if the market expand and hydrogen production technology is developed [35].

2.2. The Storage Challenge of Hydrogen

Hydrogen has a very high energy content by weight (about three times more than gasoline), but it has a very low energy content by volume (liquid hydrogen is about four times less than gasoline). This presents significant challenges to storing the large quantities of hydrogen that will be necessary in the hydrogen energy economy. Current research on future storage technology includes metal hydrides [36], metal organic frameworks [37], nanostructures [38] and chemical compounds [39]. Among the chemical hydrogen storage materials, complex hydrides such as boron hydrides are regarded as the most promising storage systems by virtue of their high gravimetric/volumetric hydrogen storage capacities [4]. However, the hydrogen stored chemical hydrides needs management of the heat produced in the hydrogen-releasing reaction and also dispose of the byproducts or “spent fuel,” created when the hydrogen is released. To achieve this several new chemical approaches have been investigated such as solvolysis, hydrogenation and dehydrogenation reactions[33].

Sodium borohydride (NaBH₄, SB) and ammonia borane (NH₃BH₃, AB) are two promising boron hydrides which, as hydrogen storage materials and fuel of the direct liquid-feed fuel cell, have attracted much attention since the early 2000s [40]. The potential utilization of SB as a hydrogen storage material [41] and as a fuel of direct fuel cell [42] were shown and also many papers showing the increasing interest in NaBH₄ have been published [43]. An efficient reaction of NaBH₄ and water for the production of hydrogen gas to be used as fuel for a variety of fuel cells. Moreover, the hydrolysis of SB is of interest in connection with the use of the compound as a reducing agent in aqueous solutions [44]. In the presence of a metal catalyst, the reaction is accomplished to fasten and optimize the generation of hydrogen at moderate temperature [45] Eq.(2). A enough chemical support lets out the water throughout the reaction bed and prevents the formation of solid sodium metaborate.



However, in November 2007, US-DOE reported that NaBH₄ is not recommended for on-board vehicle hydrogen storage because the NaBH₄ does not meet US DOE criteria in terms of storage capacity, spent fuel recycling and cost [46]. The conclusion of report is not completely negative since it consistently remarks that the improvements obtained for NaBH₄ can benefit NH₃BH₃.

AB has received considerable interest given its stability and commercial availability. Ammonia borane is a solid at room temperature, stable in air and water and contains 190 g/kg (100–140 g/L) hydrogen. Figure 1 shows that if a large portion of the hydrogen can be liberated, AB has a higher gravimetric density than most other reported chemical systems. In addition to the hydrogen capacity, stability has resulted in much more interest in studying ammonia borane as a hydrogen storage material [47]. AB is a tetragonal white crystal structure at room temperature with a melting point of > 110 °C, having a staggered conformation with a B–N bond

distance of 1.564(6) Å, B–H bond distance of 0.96(3)–1.18(3) Å, and N–H bond distance of 0.96(3)–1.14(2) Å [48]. The solid state structure shows short BH/HN intermolecular contacts; the hydridic hydrogen atoms on boron are 2.02 Å away from the protic hydrogen atoms on nitrogen of an adjacent molecule, a distance less than the Van der Waals distance of 2.4 Å, implying an interaction constituting a dihydrogen bond [49].

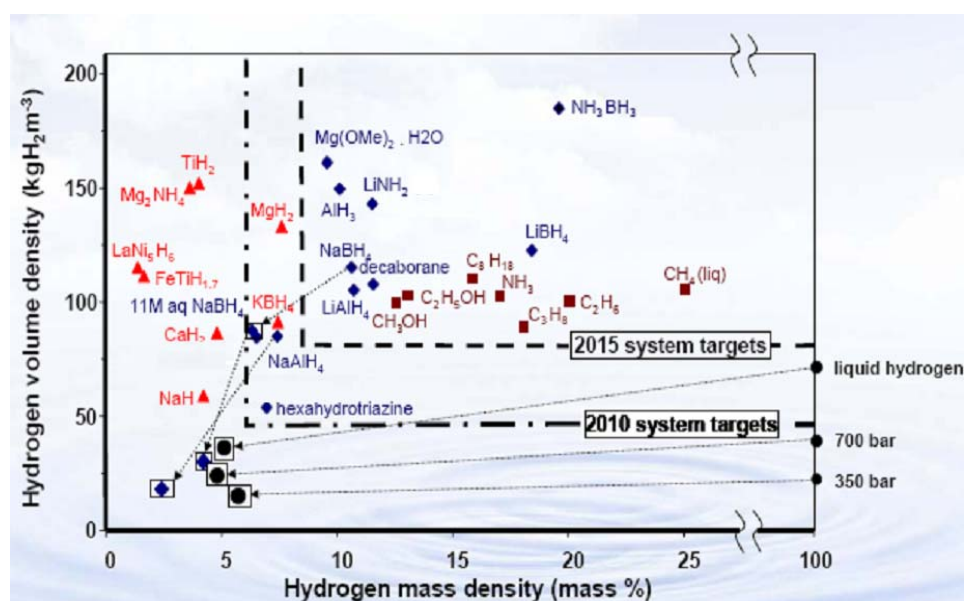
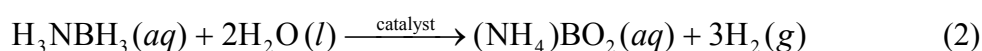


Figure 1. Representation of gravimetric and volumetric densities of different hydrogen storage materials [50].

Thus far, the hydrogen generation from AB has been achieved by thermolysis, [51] solvolysis (hydrolysis or methanolysis), [52,53] and dehydrogenation [54]. Among the methods, the catalytic hydrolysis of AB appears to be the most convenient one for portable hydrogen storage applications [55], as it provides the release of 3 moles of H₂ per mole of AB in the presence of a suitable catalyst at ambient temperatures according to Eq.(3).



The hydrolysis of AB in the presence of a suitable catalyst supplies 3 moles of hydrogen per mole AB at room temperature Eq. (3). The few studies on AB hydrolysis [56,57] have been performed to find the most efficient catalysts for hydrogen generation. Moreover, the kinetics of hydrogen generation from catalytic hydrolysis reactions can be studied depending on different catalyst and substrate concentration and temperature. According to the results, the activation parameters (Arrhenius activation energy (E_a), activation enthalpy (ΔH^\ddagger) and activation entropy (ΔS^\ddagger) of catalytic hydrolysis calculated from the kinetic data. Under light of these information, detailed controllable mechanism of hydrogen generation reactions is obtained.

CHAPTER 3

TRANSITION METAL(0) NANOCCLUSERS AS CATALYST

3.1. Transition Metal(0) Nanoclusters

Transition metal(0) nanoclusters are nearly monodispersed particles and generally less than 10 nm (10-100 Å) in diameter [58] have generated severe attention over the past decade. The most important reason for this is that these particles and their properties stretch out somewhere between those of bulk and single-particle species [59]. Transition metal nanoclusters have many interesting potential uses including quantum dots [60], quantum computers [61] and devices [62], chemical sensors [63], light emitting diodes [64], industrial lithography [65], and photochemical pattern applications [66]. Nanoclusters also have noteworthy potential as new type of catalysts and they also have higher activity and selectivity than standard metal counterparts [67].

The nanoclusters have distinctive physical and chemical properties since a large proportion of nanoclusters' metal atoms be positioned on the surface, and that these surface atoms do not unavoidably arrange themselves in the same way that those in the bulk do [68]. Moreover, metal nanoclusters no longer pursue classical physical laws as all bulk materials do. They are properly to be considered by means of quantum mechanics. The melting point of a solid chemical compound in a classical sense is a constant under distinctive conditions not so on the nanoscale.

The melting point falls down while the size of nanocluster reduces which can be seen from Figure 2.

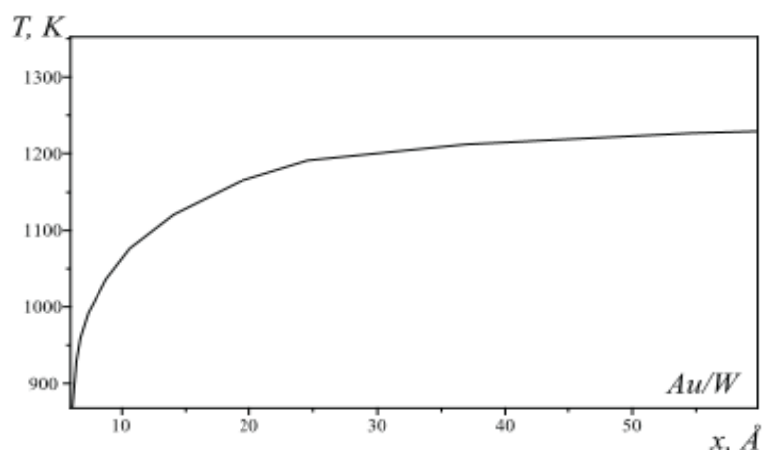


Figure 2. Melting point behavior of gold nanoparticles [69].

For the size confidence of physical and chemical properties, the phrase ‘size quantization’ has been called. Nanoclusters, consisting of metal atoms only, modify their physical properties impulsively from a distinct size on. Particle size of metal nanoparticle is below than 10 nm be evidence for typical quantum size behaviour, even at room temperature due to the continuation of discrete electronic energy levels and the loss of overlapping electronic bands, the characteristic of a bulk metal (Figure 2). Therefore, they are also named as artificial big atoms and are to be seen as a link between bulk metals and small molecular clusters [81].

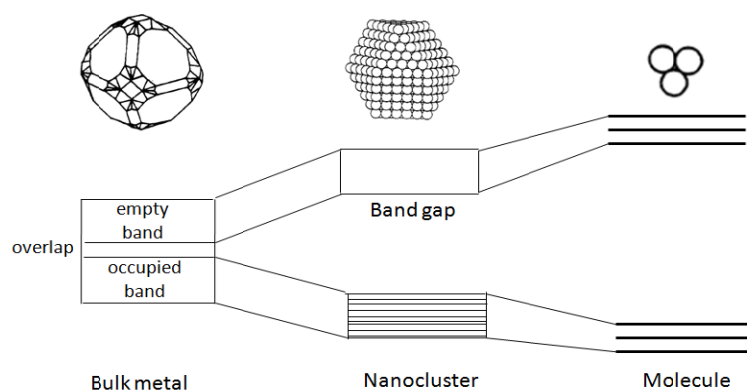


Figure 3. The change of the electronic states in (a) a bulk metal particle (b) a large cluster of cubic close packed atoms, (c) simple triatomic cluster [70].

Besides the exciting electronic changes on the way from bulk to molecule or vice versa, other properties change too. These atomic-like electron energy levels are formed due to charge-carrier confinement (quantum confinement) in three dimensions and result in an increase (blue shift) of the effective band gap compared to that of the corresponding bulk materials [71]. This change can be exemplified by gold when size of bulk gold is decreased to 50 nm in solution, the yellow color disappears and turns to blue color, further reductions consequence in purple color and finally red colors [59]. In contrast to the bulk gold inactive as catalyst, many studies have been performed by using gold nanoparticle in catalytic reactions [72].

3.2. Stabilization of Transition Metal(0) Nanoclusters

Transition metal nanoclusters are simply kinetically stable and thermodynamically unstable in solution to agglomerate into bulk metal. In this regard, metal nanoclusters in solution would be attracted to each other by van der Waals forces in the deficiency of repulsive forces. The stabilization of the metal nanoclusters is the crucial step to avoid agglomeration and to manage the size growth of them for the research of long lived transition metal catalysts established in Figure 4.

functional groups of polymer and metal and also polymer chain can coordinate to the surface of metal nanoclusters at multiple sites [78]. The arrangement of polymer stabilized metal nanoclusters can be illustrated in Figure 7, where the polymers were thought to adsorb physically on the surface of metal nanoclusters [79]. Detailed characterization studies of the adsorbed polymer have demonstrated that the polymers can coordinate to the metal forming rather strong chemical bonds. The polymer molecule can coordinate to the metal particle at multiple sites.

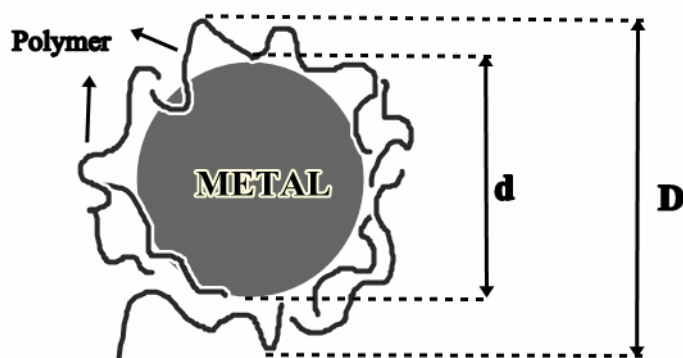


Figure 7. Structure model of polymer-stabilized metal nanoclusters [80].

Two forms are proposed for the stabilization of the metal nanocluster by a polymer as shown in Figure; (8a) the stabilization of each nanoclusters by one polymer chain (the widely accepted one, Figure 8a) the stabilization of many nanoclusters by one polymer chain (Figure 8b). As clearly seen for the both models, there still exists a large catalytically active exposed surface which is essential for heterogeneous catalytic applications.

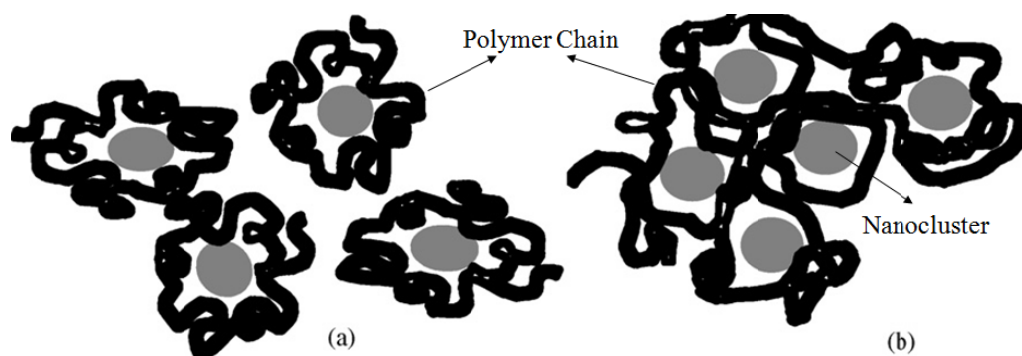


Figure 8. a) each nanocluster stabilized by one polymer chain (the widely accepted one); b) many nanoclusters stabilized by one polymer chain.

The selection of polymer as a stabilizer is concluded by concern of the solubility of the metal colloid precursor, the medium of alternative, and the ability of the polymer to stabilize the reduced metal particles in the colloidal state [59]. For this reason, it is vital to explore a wide diversity of protective polymers for their skill to stabilize metal nanoclusters. The use of polymeric matrix as stabilizer gets better some properties of the nanoclusters such as the solubility, thermal stability and catalytic activity [81].

3.2.3. Electrosteric Stabilization

Electrosteric stabilization is the combination of the electrostatic and steric stabilization keeps the stable metal nanoclusters [82]. This type of stabilization is frequently accomplished by using ionic surfactants. The source of the electrostatic constituent can be a net charge on the particle surface (Figure 9a) and/or charges cooperated with the polymer attached to the surface (i.e. through an attached polyelectrolyte) (Figure 9b). It is also probable to have combinations of reduction stabilization with both steric and/or electrostatic stabilization. The arrangement of depletion and steric stabilization is very common if there are high concentrations of free polymer in the distribution medium [83].

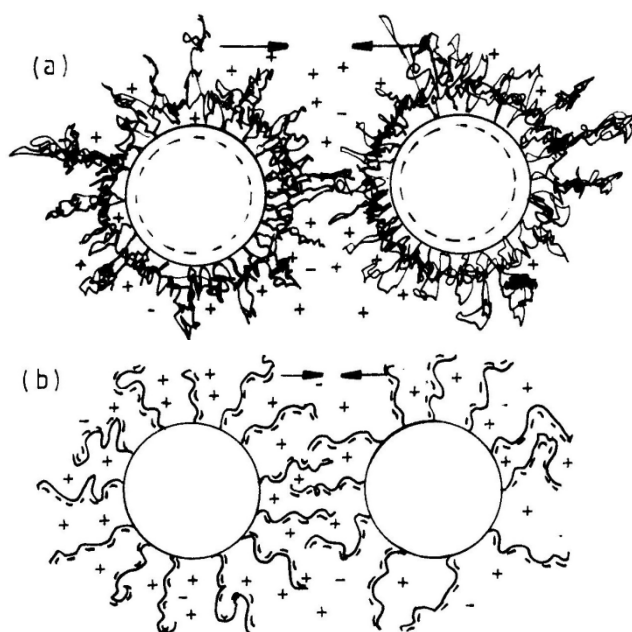


Figure 9. Representations of electrosteric stabilization: (a) charged particles with nonionic polymers; (b) polyelectrolytes attached to uncharged particles.

3.3. Synthesis of Transition Metal(0) Nanoclusters

The major goal for catalysis research in this century is to develop the reproducible modern transition metal nanoclusters syntheses instead of traditional colloids. In this regard, these nanoclusters should have specific size(1-10 nm), well-defined surface composition, reproducibility of synthesis and properties, and also be isolable and redissolvable [84].

The syntheses of transition metal nanoclusters has inspired widespread study focused toward getting control of particle size, shape, and composition under gentle conditions which are generally grouped into two main categories: ‘*bottom-up*’ and ‘*top-down*’. If researches based on building up from atomic or molecular precursors and they come together to form clusters, process is named as ‘*bottom-up*’ [85]. On the other hand, the nanoscale is reached by physically tearing down larger building blocks which is known ‘*top-down*’ but the top-down approach acquiesces poor

dispersions when the distribution of particle size is larger typically than 10 nm and also catalytic activity of catalyst prepared by this method is not reproducible because of irreproducible synthesis of metal nanoclusters [85]. On the other hand, the bottom-up approach is more convenient because of the possibilities to control the properties such as size and shape of the catalyst, catalytic reaction stoichiometry, surface area, pore size, and surface decoration) of the final product [86].

In bottom-up route, wet chemical techniques are used to prepare the transition metal nanoclusters which includes five synthetic methods generally. These are (1) chemical reduction of transition metal complexes [87], (2) thermal or photochemical decomposition [88], (3) decomposition of organometallics [89], (4) metal vapour synthesis [90], and (5) electrochemical reduction [91]. Among these preparation techniques, the chemical reduction of transition metal salts is the most convenient and efficient method in the laboratory conditions to prepare transition metal nanoclusters as previously mentioned properties above.

3.4. Transition Metal(0) Nanoclusters in Catalysis

3.4.1. General Concepts of Catalysis

Catalyst is considered as chemical compound capable of directing and accelerating thermodynamically feasible reactions while remaining unaltered at the end of the reaction. The phenomenon occurring when a catalyst acts is termed *Catalysis*. There are many types of catalyst used in the industrially or specifically important reactions including transition metal salts, zeolites, organic molecules, lewis acids, enzymes and organometallic compounds. However, catalysis can be categorized mainly into three groups as heterogeneous, homogeneous, and biological to make simplification as shown in Figure 10. *Catalysis* is called as homogeneous when the catalyst is soluble in the reaction medium while heterogeneous when the catalyst is existing in a phase distinctly different from the phase of the reaction

medium [92]. The heterogeneous catalyst is usually in the solid phase while the reactants are either gaseous or liquid. The gas or liquid molecules bind temporarily to the atoms at the surface of the catalyst, which allows the breaking of their internal bonds to more and this of catalysis is widely used in industrial manufacture of chemicals because of easy separation of reaction product, reusability, stability, low-cost and low-toxicity [93]. The last group of catalysts is the biocatalysts which are called as enzymes. Enzymes are the nature's own crucial catalysts for existence of life and they have the most complex structures among three kinds of catalysts.

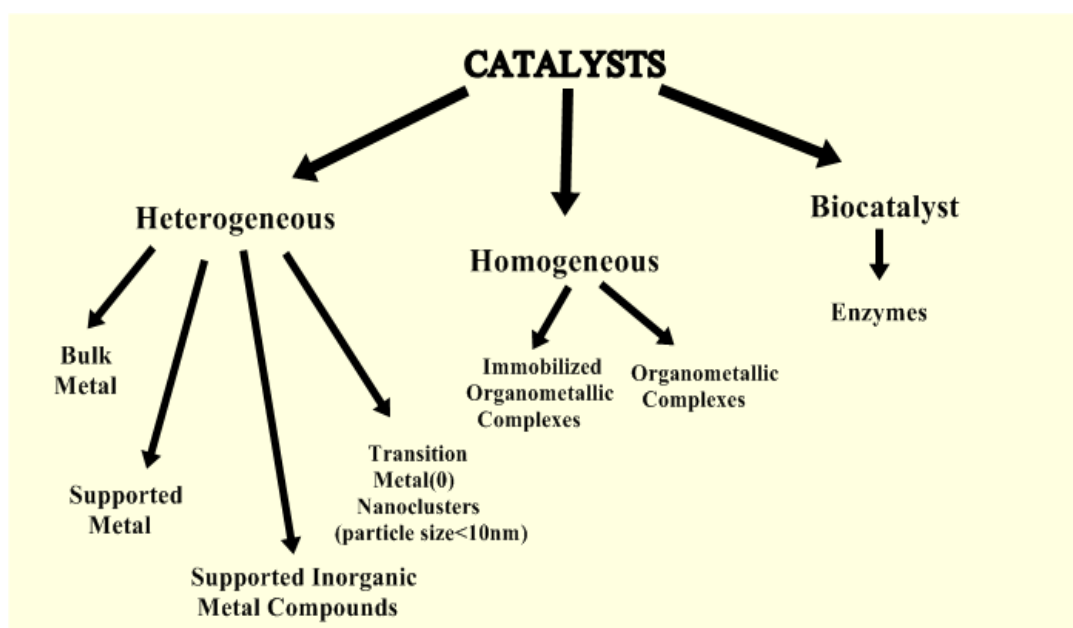


Figure 10. The classification of catalysts [94].

Catalyst can be also defined as a substance that increases a reaction rate and decrease the activation energy of the chemical reaction by providing an alternative mechanism involving a different transition state without itself being consumed in the reaction which called as transition-state theory. The energy released or absorbed by a chemical reaction is exactly the same whether a catalyst is present or not. According to the transition-state theory, the activated reactants have to be into get in touch with each other physically (collision) in which much more stabilized transition states are formed than uncatalyzed reactions that contains, in the presence of a heterogeneous catalyst, movement of reactant from one catalyst atom to next over the surface of the

catalyst, until it get in touch with another bound reactant. Therefore, the activation energy for the catalyzed reaction should be less than for the uncatalyzed reaction as the illustrated in the Figure 11[95]. However, the apparent activation energy (E_a^{apparent}) term is generally used for the activation energy of a catalytic reaction go on many steps because there are many methods to product side in this type of reactions and so there are many rate constants (k_{app}) influenced by temperature and the combination of these rate constants is named as E_a^{apparent} .

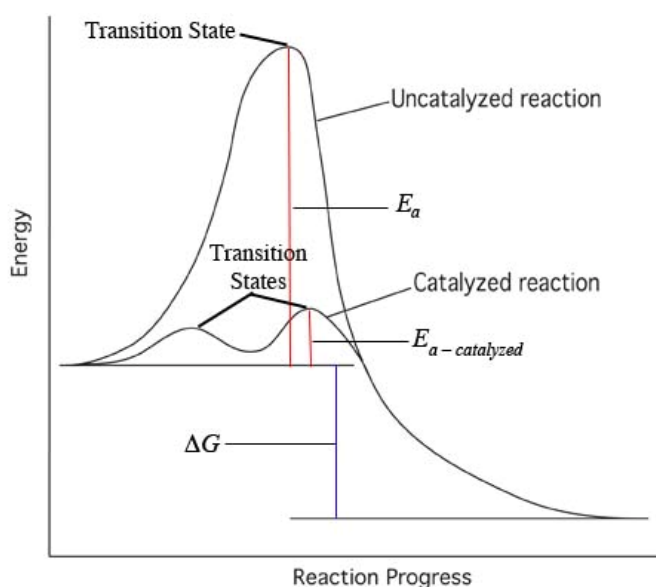


Figure 11. Schematic representation of the energetics in catalytic cycle [96].

As a conclusion, the important aspect is that the catalyst does not affect the overall entropy change of reaction but provides a new reaction pathway with lower barrier of activation. The new pathway may include many intermediates and reaction steps which form the mechanism of catalytic reaction.

3.4.2. Definitions of Catalytic Terms

The turnover frequency (TOF) and total turnover number (TTON) are two important quantities used for comprising efficiency of catalyst. These are crucial terms in the conversion of A to B catalyzed by Q with rate v , Eq.1;



The catalytic turnover frequency (TOF), N , is the catalytic turnover number per unit time and indicates efficiency of a catalyst. TOF is given by Eq.2;

$$N = \frac{v}{[Q]} \quad (4)$$

Total turnover number (TTON) equals to the number of moles of product per mole of catalyst Eq. (3); this equation gives the number of the total catalytic cycles that a catalyst can run through before deactivation.

$$TTON = (TOF) \times (time) = \frac{\text{mole of product}}{\text{mole of catalyst}} \quad (5)$$

Selectivity is the last and also crucial property of the catalyst that ought to be considered in the performance of any catalyst. A selective catalyst gives a high proportion of the desired product with minimum amount of side products. By this way, selective catalysts help to reduce waste, the work-up equipment of a plant, and ensure use of the feedstocks efficiently.

3.4.3. The Characterization Methods of Transition Metal Nanoclusters

Numerous characterization methods are utilized to study nanocluster properties according to many parameters such as composition, preparation method, heat treatments, environmental variables, supports and so on. In order to entirely understand the physico-chemical behaviour of metal nanoclusters and their properties, many complementary methods must be used to work out the many parameters engaged [97]. *UV-visible spectroscopy* [98] has been used to assure the whole reduction of the precursor compound. Such observations done by UV-Vis

spectroscopy rely on the disappearing of an absorption of the metal precursor and raising of a new absorption feature for the nanoclusters [99]. *Infrared (IR)* spectroscopy has been used to investigate probable interactions between the metal and any other reagents used in the reaction [100]. *X-ray diffraction (XRD)* is used to display which elements are existed in the sample, to obtain information about their oxidation states, and to decide the crystallographic structure of samples and permit an precise analysis of diffraction line shape, the extraction of relevant information relating to crystallite size, crystallographic imperfections as well as compositional and chemical inhomogeneties [101].

Among the imaging methods, the most widely utilized and vital technique for the characterization of nanoparticles is *transmission electron microscopy (TEM)* and *high resolution transmission electron microscopy (HRTEM)*. TEM is used to establish particle morphology and a quantitative explanation of the particle size distribution whereas HRTEM is often used in order to recognize the crystallinity of the particles. Even for very small sized particles and lattice structure could be examined [100]. In these techniques, a high voltage electron beam passes through a very thin sample, and the sample areas that do not permit the channel of electrons form an image to be presented. Other commonly used methods for the characterization of metal nanoparticles can be summarized as follows: *X-ray photoelectron spectroscopy (XPS)*; is a semi-quantitative technique used for the determination of the surface chemical properties of the materials. The oxidation state of the metal atom on the surface of metal nanoclusters can be determined via XPS which is very important issue in heterogeneous catalysis [102]. To a less extent the following methods are used for the characterization of metal nanoparticles: scanning electron microscopy (SEM), elemental analysis (ICP-OES). An overall picture of the methods most commonly used in the characterization of metal nanoparticles are given in Figure 12[103].

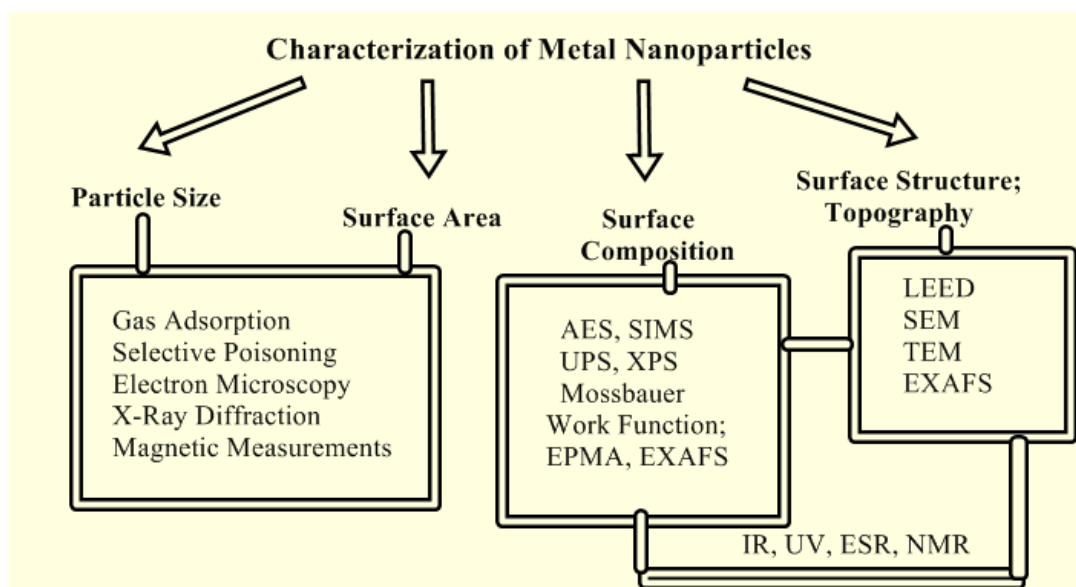


Figure 12. The common methods of characterization of transition metal nanoclusters.

3.4.4. Surface Area Effect of Heterogeneous Catalysis in Catalytic Activity

The activity of the catalyst is openly related to its surface area, and so decreasing the particle size of the catalyst is a hopeful approach to increase the catalytic activity. In this regard, the metal nanoclusters are more active catalysts than the respective bulk metal counterparts because large percentage of atom spreads out on the surface of nanoclusters [75].

Transition metal nanoclusters gain great interest at present due to their unique chemical and physical properties result from their nano-dimensions. [104]. Metal clusters have a completely regular outer geometry which are designed full-shell or magic number clusters. Each metal atom pass ons some degree of extra stability to full-shell clusters because of the maximum number of nearest neighbors. The number of atoms enhances while the percentage of the surface atoms reduces as illustrated in Figure 13.






Full-Shell "Magic Number" Clusters					
Number of shells	1	2	3	4	5
Number of atoms in cluster	M ₁₃	M ₅₅	M ₁₄₇	M ₃₀₉	M ₅₆₁
Percentage surface atoms	92%	76%	63%	52%	45%

Figure 13. Inverse relationship between the total number of atoms in full shell clusters and the percentage of surface atoms in representation in hexagonal close-packed full-shell ‘magic number’ clusters [105].

In the literature, the studies are reported in the literature expectedly demonstrate that transition metal nanoclusters are more active catalyst than their bulk-counterparts in various reactions [106].

CHAPTER 4

EXPERIMENTAL

4.1. Materials

Iron(III) chloride hexahydrate (98%), sodium borohydride (NaBH₄, SB, 98%), polyethylene glycol (PEG, average molecular weight = 2000 g.mol⁻¹), ethylene glycol (EG), borane ammonia complex (H₃NBH₃, AB, 97 %) were purchased from Aldrich[®]. Deionized water was distilled by water purification system (Milli-Q System). All glassware and Teflon coated magnetic stir bars were cleaned with acetone, followed by copious rinsing with distilled water before drying in an oven at 150 °C.

4.2. Preparation of PEG Stabilized Iron(0) Nanoclusters

PEG stabilized iron(0) nanoclusters were prepared from the reduction of iron(III) chloride by a mixture of SB and AB in the presence of PEG in ethylene glycol solution at 80 °C under continuous argon flow by using our own special experimental setup (Figure 14). In a 250 mL three-necked round bottom flask, 135 mg (0.5 mmol) of FeCl₃.6H₂O and 62 mg (1.0 mmol monomer unit) of PEG were dissolved in 15 ml of ethylene glycol (molar ratio of PEG to Fe is 2). The resultant mixture in ethylene glycol was refluxed by continuous stirring at 1000 rpm at 80 °C under continuous argon flow. Then, a mixture of 142.0 mg of SB and 32.0 mg AB dissolved in 1.0 mL water was quickly injected into the metal-polymer solution at 80 °C. The abrupt color change from pale yellow to black in less than 10 seconds indicates the completion of the reduction of iron(III) to iron(0) nanoclusters. It is

4.3. Characterization of PEG Stabilized Iron(0) Nanoclusters

UV-Vis electronic absorption spectra of precursor metal salt and PEG stabilized iron(0) nanoclusters were recorded in aqueous solution on Varian-Carry100 double beam instrument. Scanning electron microscope (SEM) and electron diffraction X-ray (EDX) data were acquired using a Zeiss EVO40 environmental SEM that is equipped with a LaB6 electron gun, a vacuum SE detector, an elevated pressure SE detector, a backscattering electron detector (BSD), and a Bruker AXS XFlash 4010 detector. Samples for SEM and EDX analysis were prepared by grinding the powder samples into fine particles and mechanically dispersing them on an electrically conductive carbon film which was placed on an aluminum sample holder. No additional coatings or dispersive liquids were used for the SEM and EDX sample preparation. SEM images were obtained using a vacuum SE detector where electron acceleration voltage of the incident beam was varied within 10-20 kV and the samples were kept typically at $\leq 5 \times 10^{-5}$ Torr inside the SEM. All of the EDX data were collected using an electron acceleration voltage of 20 kV and a working distance of 15 mm. X-ray diffraction (XRD) pattern was recorded on a Rigaku Miniflex diffractometer with $\text{CuK}\alpha$ (30 kV, 15 mA, $\lambda = 1.54051 \text{ \AA}$), over a 2θ range from 5 to 90 ° at room temperature. Transmission electron microscope (TEM) images were obtained using a JEM-2100 (JEOL) instrument operating at 200 kV. The nanoclusters solution prepared as described in the section 4.2 was centrifuged at 6000 rpm for 10 min. Then, the nanoclusters sample was redispersed in 5 mL methanol. One drop of the diluted colloidal solution was deposited on the silicon oxide coated copper grid and evaporated under inert atmosphere. Samples were examined at magnifications between 100 and 800k. Particle size of the nanoclusters is calculated directly from the TEM image by counting non-touching particles. Size distributions are quoted as the mean diameter \pm the standard deviation. FT-IR spectra were recorded on a Bruker Vertex 70 spectrophotometer by an Attenuated Total Reflectance (ATR) modul. The iron contents of the PEG stabilized iron(0) nanocluster samples after centrifugation were

determined by ICP-OES (Inductively Coupled Plasma Optical Emission Spectroscopy, Leeman-Direct Reading Echelle) after each sample was completely dissolved in the mixture of HNO₃/HCl (1/3 ratio). For ICP-OES analysis, a calibration curve was prepared by measuring the absorption of 0, 1, 2, 5, 10 and 20 ppm of standard solution of Fe. Then, the absorption of the samples of PEG stabilized iron(0) nanoclusters was measured and the Fe content of the samples was determined from the calibration curve.

4.4. Testing the Catalytic Activity of PEG Stabilized Iron(0) Nanoclusters in the Hydrolysis of AB

The catalytic activity of PEG stabilized iron(0) nanoclusters were tested in the hydrolysis of AB by measuring the rate of hydrogen generation. To determine the rate of hydrogen generation, a jacketed reaction flask (50.0 mL) containing a Teflon-coated stir bar was placed on a magnetic stirrer (Heidolph MR-301) and thermostated to 25.0 ± 0.5 °C by circulating water through its jacket from a constant temperature bath. Then, a graduated glass tube filled with water was connected to the reaction flask to measure the volume of the hydrogen gas to be evolved from the reaction (Figure 15). Next, aliquot of nanoclusters in 10 mL water was transferred to the jacketed reaction flask. Firstly, PEG stabilized iron(0) nanoclusters were employed as catalyst in the hydrolysis of SB. In a typical experiment for the hydrolysis of SB, 76.0 mg (2.0 mmol) of NaBH₄ was dissolved in 1.0 mL water and injected into the nanoclusters solution in the jacketed reaction flask at 25.0 ± 0.5 °C. After hydrogen generation from the hydrolysis of SB was completed in the presence of PEG stabilized iron(0) nanoclusters, 63.0 mg of AB dissolved in 1.0 mL water was injected into the reaction solution without any purification. The hydrogen generation from both hydrolyses in the presence of PEG stabilized iron(0) nanoclusters were measured by every minute until no hydrogen gas evolution was observed.

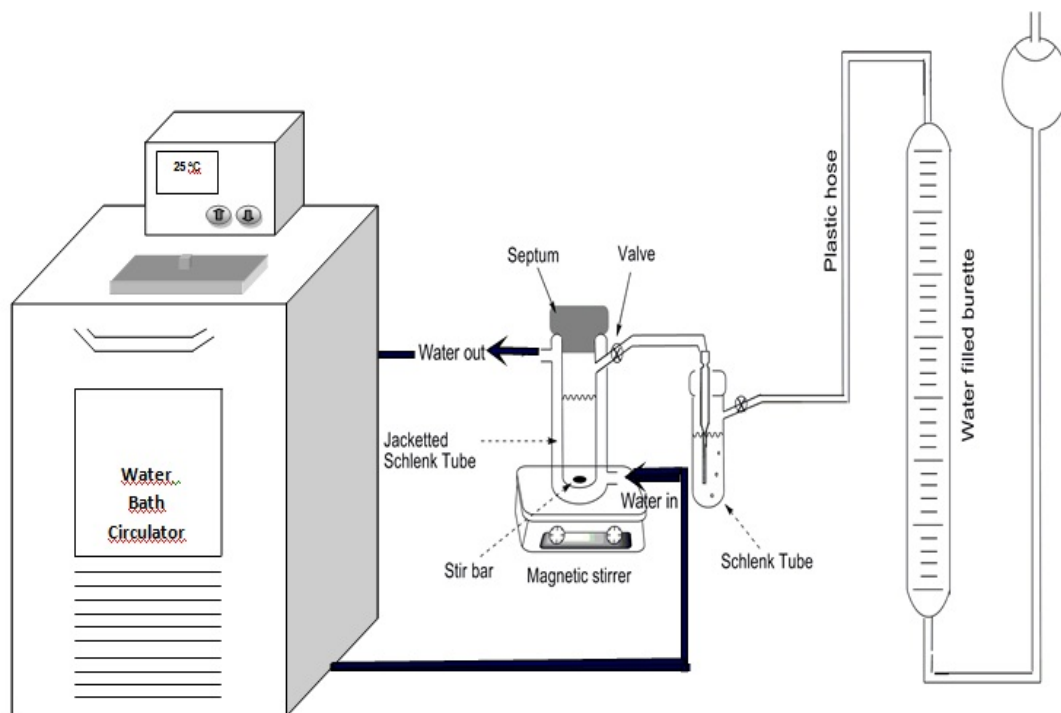


Figure 15. The experimental setup used in performing the catalytic hydrolysis of ammonia borane and measuring the hydrogen generation rate.

4.5. Quantification of the Liberated NH_3 Gas

The gas generated from the catalytic hydrolysis of AB was passed through 25 mL standardized solution of 0.001 M HCl at room temperature. After gas generation was ceased, the resulted solution was titrated with standard solution of 0.01 M NaOH by using phenolphthalein acid-base indicator. The quantity of the liberated ammonia gas was calculated from the difference between two HCl solutions before and after the reaction.

4.6. Effect of PEG Concentration on The Catalytic Activity of Iron(0) Nanoclusters in The Hydrolysis of AB

In order to determine the effect of PEG concentration on the catalytic activity of iron(0) nanoclusters in the hydrolysis of AB (200 mM), catalytic activity tests were performed at 25.0 ± 0.5 °C starting with various PEG/Fe ratio in the range of 1-10 by keeping the initial concentrations of Fe, SB and AB constant at 0.5, 4.0 and 1.0 mmol, respectively. In all the experiments, the total volume of catalytic solution was kept constant at 10.0 mL and all experiments were performed following the same procedure as described in the section 4.2.

4.7. Kinetics of Hydrolysis of AB Catalyzed by PEG Stabilized Iron(0) Nanoclusters

In order to determine the rate law for catalytic hydrolysis of AB catalyzed by PEG stabilized iron(0) nanoclusters, three different sets of experiments were performed as described in the section 4.2. Firstly, the AB concentration was kept constant at 200 mM and the Fe concentration was varied in the range of 5.0-30.0 mM at 25.0 ± 0.5 °C. Secondly, the iron concentration was kept constant at 25.0 mM and the AB concentration was varied in the range of 0.1-2.0 M. Finally, the catalytic hydrolysis reaction of AB in the presence of PEG stabilized iron(0) nanoclusters was performed at constant catalyst (25.0 mM) and constant AB (200 mM) concentration by varying the temperature in the range of 15.0-35.0 °C in order to obtain the activation energy.

4.8. Catalytic Lifetime of PEG Stabilized Iron(0) Nanoclusters in the Hydrolysis of AB

In order to determine the catalytic lifetime of PEG stabilized iron(0) nanoclusters in the hydrolysis of AB, the total turnover number (TTON) was measured. In this experiment, 10.0 mL of aqueous solution containing PEG stabilized iron(0) nanoclusters catalyst (15.0 mM Fe) and 500 mM AB (160 mg) at 25.0 ± 0.5 °C. After conversion of all AB present in the solution, checked by monitoring the stoichiometric H₂ gas evolution (3.0 mol H₂/mol H₃NBH₃), a new batch of 160.0 mg of AB was added and the reaction was kept going in this way until no hydrogen gas evolution was observed.

4.9. Reusability of PEG Stabilized Iron(0) Catalyst in The Hydrolysis of AB

A reusability test started with a 10.0 mL of aqueous solution containing PEG stabilized iron(0) catalyst (15.0 mM Fe) and 200.0 mM AB (62 mg) at 25.0 ± 0.5 °C. Next, PEG stabilized iron(0) nanoclusters were isolated from the reaction solution magnetically by using a magnet when the hydrolysis was completed in each run. The magnetically recovered PEG stabilized iron(0) nanoclusters were redispersed in 10.0 mL water and a new catalytic run was started by addition of new batch of 62.0 mg AB as described in the section 4.2.

CHAPTER 5

RESULTS AND DISCUSSION

5.1. Preparation and Characterization of PEG Stabilized Iron(0) Nanoclusters

PEG stabilized iron(0) nanoclusters were prepared from the reduction of iron(III) chloride by a mixture of SB and AB in the presence of polyethylene glycol (PEG) in ethylene glycol solution under inert atmosphere at 80 °C. In this protocol, PEG serves as stabilizer to prevent the agglomeration and oxidation of iron(0) nanoclusters in solution, which are highly reactive with respect to both agglomeration and oxidation. The mixture of SB and AB is used to reduce the metal precursor in the presence of PEG because the use of sole SB as a reducing agent results in the agglomeration of nanoparticles, a fact which has previously been observed by Xu *et al.* [19], and this agglomeration causes a decrease in catalytic activity (see later) [107]. The abrupt color change from pale yellow to black was observed within 10 seconds after addition of reducing agents into the solution of metal precursor indicating the reduction of iron(III) to iron(0). The conversion of iron(III) chloride to iron(0) nanoclusters was nicely followed by taking UV-visible electronic absorption spectra of the reaction solution during the preparation of PEG stabilized iron(0) nanoclusters. Upon addition of the mixture of SB and AB into the solution, the absorption band of iron(III) ions at 292 nm [108] disappeared (Figure 16) and the characteristic absorption continuum for iron(0) nanoclusters was observed [109].

were counted for the construction of histogram (Figure 19b). The particle size of PEG stabilized iron(0) nanoclusters ranges from 4.0 nm to 8.5 nm with a mean value of 6.3 nm.

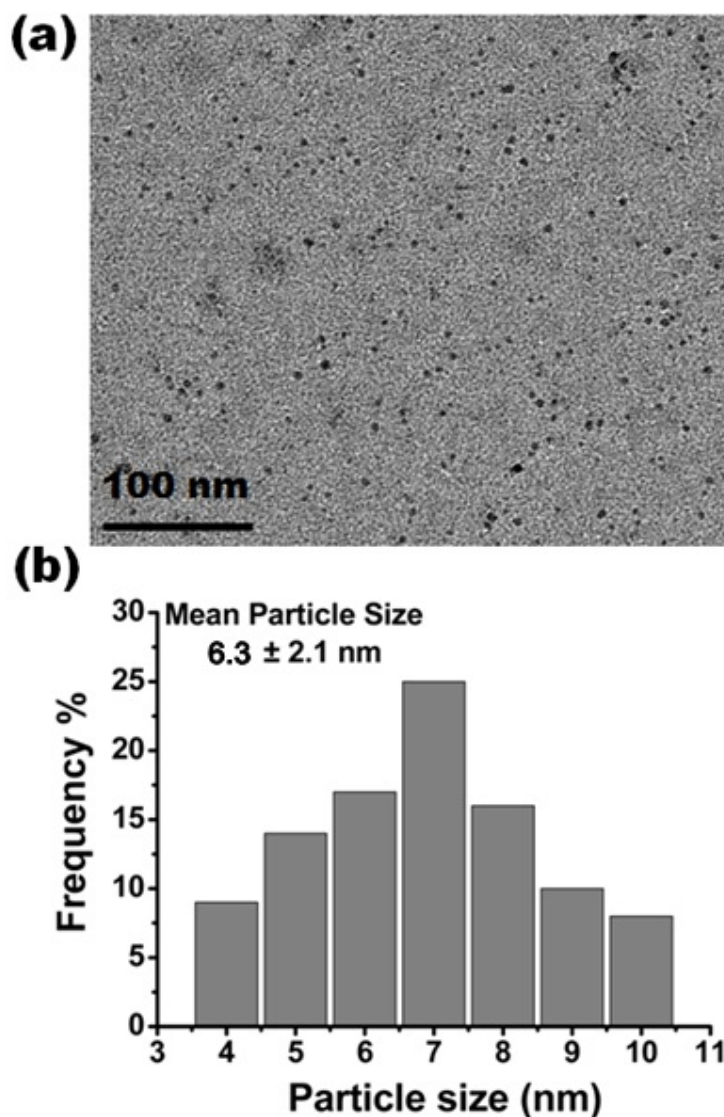


Figure 19. a) Low resolution TEM image b) corresponding particle size histogram of PEG stabilized iron(0) nanoclusters.

Figure 20 shows the HRTEM image of the PEG stabilized iron(0) nanoclusters taken from the methanol solution. As clearly seen from the HR-TEM image, well-dispersed and nearly spherical nanoparticles were obtained without any

agglomeration after reduction of iron(III) chloride by SB-AB mixture in the presence of PEG.

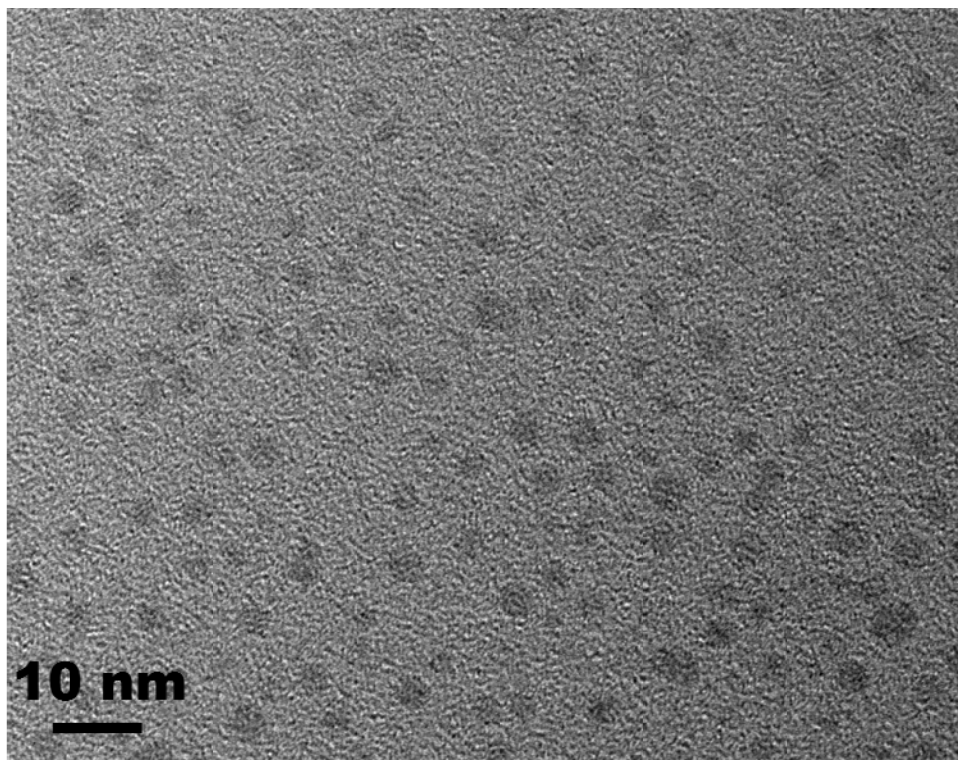


Figure 20. HRTEM image of the PEG stabilized iron(0) nanoclusters taken from the methanol solution.

Figure 21. X-ray diffraction patterns of PEG stabilized iron(0) nanoclusters prepared from the reduction of iron(III) chloride by a) sodium borohydride and b) a mixture of sodium borohydride and ammonia borane.

Figure 22a shows the plots of volume of hydrogen versus time during the hydrolysis of AB catalyzed by PEG stabilized iron(0) nanoclusters at different PEG/Fe ratio. The inset in Figure 22a shows the plot of the hydrogen generation rate versus the [PEG]/[Fe] ratio for the hydrolysis of AB at 25.0 ± 0.5 °C. As clearly seen from the Figure 22a, the hydrogen generation rate decreases with the increasing concentration of polymeric stabilizer after the ratio of 2 as expected [110]. The lower activity of iron(0) nanoclusters in the presence of one fold PEG was due to the agglomeration of the particles during the catalytic reaction. Additionally, TEM images of the PEG stabilized iron(0) nanoclusters at different PEG/Fe ratio of 2, 3, or 4 given in Figure 22b, 22c and 22d, respectively, show that the increasing amount of PEG stabilizer results in the formation of larger nanoclusters composed in the polymer matrix by increasing the number of iron atoms. Therefore, the activity of the iron(0) nanoclusters in the hydrolysis of AB decreases as a result of reduction of active surface area. The [PEG]/[Fe] ratio of 2 leads to the formation of small nanoparticles stabilized by polymer. By considering both the catalytic activity and stability of the nanoclusters in the hydrolysis of AB, the [PEG]/[Fe] ratio of 2 was used for all the kinetic experiments.

After testing the activity of PEG stabilized iron(0) nanoclusters in the hydrolysis of AB, we performed a detailed kinetic study on the hydrolysis of AB. Figure 24a shows the plots of the volume of hydrogen generated versus time during the catalytic hydrolysis of 200.0 mM AB solution in the presence of iron(0) nanoclusters starting with different catalyst concentration at 25.0 ± 0.5 °C. The initial rate of hydrogen generation was determined from the initial, nearly linear portion of each plot for different catalyst concentration. The hydrogen generation rate reached up to $36.4 \text{ mL H}_2 \cdot \text{min}^{-1}$ for the hydrolysis of AB in the presence of iron(0) nanoclusters catalyst (25.0 mM Fe) corresponding to a turnover frequency of 6.5 min^{-1} , which is the highest value ever reported for the hydrolysis of AB using iron catalyst. Figure 24b shows the plot of hydrogen generation rate versus iron concentration, both in logarithmic scale. The line obtained has a slope of $0.98 \approx 1.00$ indicating that the hydrolysis of AB catalyzed by PEG stabilized iron(0) nanoclusters is first order with respect to the catalyst concentration.

The effect of substrate concentration on the hydrogen generation rate was also studied by performing a series of experiments starting with different initial concentrations of AB while keeping the catalyst concentration constant at 25.0 mM Fe at 25.0 ± 0.5 °C (Figure 25a). It is clearly seen from the slope of the rate versus concentration plot given in Figure 25b that the hydrogen generation from the catalytic hydrolysis of AB in the presence of PEG stabilized iron(0) nanoclusters is a first order reaction with respect to the AB concentration in the range of 0.1-0.5 M AB. However, the deviation from the first order dependency is observed in the higher substrate concentration and the slope of the plot approaches to zero when the $[\text{AB}]/[\text{Fe}]$ ratio is greater than 200, that is, the hydrogen generation from the catalytic hydrolysis of AB in the presence of PEG stabilized iron(0) nanoclusters becomes pseudo-zero order with respect to the AB concentration. Consequently, the rate law for the hydrolysis of AB catalyzed by PEG stabilized iron(0) nanoclusters can be found as a pseudo first order given as Eq.(6);

$$-\frac{3 d[\text{AB}]}{dt} = \frac{d[\text{H}_2]}{dt} = k' \cdot [\text{Fe}] \text{ where } k = k' \cdot [\text{AB}] \quad (6)$$

The hydrolysis of AB catalyzed by PEG stabilized iron(0) nanoclusters was carried out at various temperature in the range of 15.0-35.0 °C starting with the initial substrate concentration of 200 mM AB and an initial catalyst concentration of 25.0 mM Fe. Figure 26a shows the plot of volume of hydrogen generated versus time for the hydrolysis of AB in the presence of PEG stabilized iron(0) nanoclusters at five different temperatures. The values of apparent rate constant k (k_{app}) given in Table 1 for the catalytic hydrolysis of AB were obtained from the slope of each plot in Figure 26a and used to calculate the apparent activation energy (Arrhenius plot is shown in the Figure 26b): $E_a^{app} = 37.0 \pm 2.0 \text{ kJ}\cdot\text{mol}^{-1}$.

Table 1.

The values of apparent rate constant (k_{app}) for the catalytic hydrolysis of ammonia borane starting with a solution of 200 mM H_3NBH_3 and 25.0 mM PEG stabilized iron(0) nanoclusters at different temperatures, calculated from the hydrogen volume versus time data.

Temperature (K)	Rate Constant, k_{app} for hydrolysis of H_3NBH_3 $\text{mol H}_2\cdot(\text{mol Fe})^{-1}\cdot\text{min}^{-1}$
288	1.021
293	1.303
298	1.792
303	2.181
308	2.812

A catalyst lifetime experiment was performed starting with PEG stabilized iron(0) nanoclusters (15.0 mM Fe) and 500 mM AB in 10.0 mL aqueous solution at $25.0 \pm 0.5 \text{ }^\circ\text{C}$. The PEG-stabilized iron(0) nanoclusters provide 1300 turnovers over 42 hours before deactivation. The deactivation of catalyst in 42 h can be explained by the increasing viscosity and pH due to the formation of $[\text{NH}_4][\text{BO}_2]$.

Figure 27a shows the volume of hydrogen generation versus time during the reusability test of PEG stabilized iron(0) nanoclusters in the hydrolysis of AB at room temperature. During the reusability test, PEG stabilized iron(0) nanoclusters were recovered from the catalytic reaction solution after each catalytic run magnetically by using a magnet (Figure 27b). Magnetically recovery of nanoparticles has recently been demonstrated for hollow Co-B nanospindles in the hydrolysis of AB [111]. The reusability test shows that the PEG stabilized iron(0) nanoclusters retain 85 % of its initial activity after 2nd run and 48 % of its initial activity after 10th run. This decrease can be result from agglomeration of nanoclusters, oxidation of iron nanoclusters and degradation of polymer chain structure.

A proposed mechanism can be suggested for the metal catalyzed hydrolysis of AB under the light of these kinetic results where the adsorption of the AB molecule on the surface of metal catalyst via nitrogen or boron atom is occurred at the first step of the mechanism. After that, native bond between nitrogen and boron atoms is weakened on the surface of metal catalyst which is followed by the attacking of water molecules to weakened bond which should be the rate determining step because the weakening of the native bond between the N-B need high energy. Finally, the reaction of BH₃ molecules with water takes place resulting in the formation of hydrogen gas and borate species in the second step.

CHAPTER 6

CONCLUSIONS

To sum up, our study on the preparation and characterization of water soluble polymer stabilized iron(0) nanoclusters as catalyst in the hydrolysis of AB leads to following conclusions and insights:

- Water dispersible iron(0) nanoclusters having average particle size of 6.3 ± 1.5 nm can be easily generated from the reduction of iron(II) chloride by SB and AB mixture in ethylene glycol at 80 °C.
- Our protocol yields nearly spherical iron(0) nanoclusters with uniform particle size distribution in water.
- PEG stabilized iron(0) nanoclusters were stable enough in solution to be isolated as solid material and characterized by TEM, SEM, EDX, XRD, ATR-IR, ICP-OES and UV-visible electronic absorption spectroscopy.
- Powder XRD study reveals that PEG stabilized iron(0) nanoclusters prepared from the reduction of iron(III) chloride by sole SB exists in α -Fe crystalline structure which shows the lower stability and catalytic activity in the hydrolysis of AB than the amorphous ones obtained by using SB-AB mixture.
- PEG stabilized iron(0) nanoclusters show high activity both in hydrogen generation from the hydrolysis of AB at room temperature providing TOF values of 6.5 min^{-1} .
- The hydrogen generation from the hydrolysis of AB in the presence of PEG stabilized iron(0) nanoclusters is first order with respect to the catalyst

concentration. However, it shows a variation at different substrate concentrations; first order in AB concentration in the range of 0.1-0.5 M and zero order in AB concentrations higher than 0.5 M.

- PEG stabilized iron(0) nanoclusters can be recovered from the catalytic reaction solution magnetically by using a magnet and retain 85 % of their initial activity after 2nd and 48 % after 10th run.

As a conclusion, easy preparation, cost-effectiveness, magnetically recoverability and high activity of PEG stabilized iron(0) nanoclusters make them promising candidate as catalyst in hydrogen generation from the boron based chemical compounds for proton exchange membrane fuel cells under ambient conditions.

REFERENCES

- [1] Energy Information Administration, Annual Energy Outlook 2005 with Projections to 2025, [www.eia.doe.gov/oiaf/aeo/pdf/0383\(2005\).pdf](http://www.eia.doe.gov/oiaf/aeo/pdf/0383(2005).pdf), February, **2005** (last access date 20.07.2011).
- [2] Züttel, A., Borgschulte, A., Schlapbach, L., *Hydrogen as a Future Energy Carrier*, Wiley-VCH, Weinheim, **2008**.
- [3] U. S. Department of Energy, Basic Research Needs For the Hydrogen Economy, Report of the Basic Energy Sciences Workshop on Hydrogen Production, Storage and Use, www.sc.doe.gov/bes/hydrogen.pdf, May 13-15, **2003** (last access date 20.07.2011).
- [4] Schlapbach, L., Züttel, A., *Nature*, **2001**, 414, 353-358.
- [5] Aceves, S.M., Berry, G.D., Rambach, G.D., *Int. J. Hydrogen Energy*, **1998**, 23, 583-591.
- [6] Basic Research Needs for the Hydrogen Economy, Report of the Basic Energy Sciences Workshop on Hydrogen Production, Storage and Use, May 13–15, **2003**, Office of Science, US Department of Energy, <http://www.sc.doe.gov/bes/hydrogen.pdf>
- [7] Kalidindi, S.D., Indirani, M., Jagirdar, B.R., *Inorg. Chem.* **2008**, 47, 7424-7429.
- [8] Zahmakıran, M., Özkar, S., *Applied Catalyst B: Environmental*, **2009**, 89, 104-110.
- [9] A.T. Raissi, In Proceedings of the **2002** U.S. DOE hydrogen program review, <http://www.eere.energy.gov/hydrogenandfuelcellw/pdfs/32405b15.pdf>, **2002** NREL/CP-610-32405, (last access date 20.07.2011).
- [10] FY 2002 progress report, section V. Integrated hydrogen and fuel cell demonstrate/analysis, hydrogen, fuel cells and infrastructure technologies,

http://www.eere.energy.gov/hydrogenandfuelcells/pdfs/33098_sec5.pdf, 2002

(last access date 20.07.2011).

- [11] (a) Marder, T.B., *Angew. Chem. Int. Ed.* **2007**, 46, 8116-8118. (b) Stephens, F.H., Pons, V., Baker, R.T., *Dalton Trans.* **2007**, 25, 2613-2626, and references therein.
- [12] Schlesinger, H.I., Brown, H.C., Finholt, A.B., Gilbreath, J.R., Hockstra, H.R., Hydo, E.K., *J. Am. Chem. Soc.* **1953**, 75, 215-219.
- [13] Chandra, M., Xu, Q., *J. Power Sources*, **2006**, 156, 190-194.
- [14] Kalidindi, S.D., Indirani, M., Jagirdar, B.R., *Inorg. Chem.* **2008**, 47, 7424-7429.
- [15] Chandra, M., Xu, Q., *J. Power Sources*, **2006**, 159, 855-860.
- [16] Chandra, M., Xu, Q., *J. Power Sources*, **2007**, 168, 135-142.
- [17] (a) Chandra, M., Xu, Q., *J. Power Sources*, **2006**, 163, 364-370. (b) Yan, J.M., Zhang, X.B., Han, S., Shioyama, H., Xu, Q., *J. Power Sources*, **2010**, 195, 1091-1094.
- [18] (a) Kalidindi, S.D., Sayal, U., Jagirdar, B.R., *Phys. Chem. Chem. Phys.* **2008**, 10, 5870-5874. (b) Kalidindi, S.D., Indirani, M., Jagirdar, B.R., *Inorg. Chem.* **2008**, 47, 7424-7429.
- [19] Yan, J.M., Zhang, X.B., Han, S., Shioyama, H., Xu, Q., *Angew. Chem. Int. Ed.* **2008**, 47, 2287-2289.
- [20] Metin, Ö., Özkar, S., *Int. J. Hydrogen Energy*, **2011**, 36, 1424-1432.
- [21] Yan, J.M., Zhang, X.B., Han, S., Shioyama, H., Xu, Q., *Inorg. Chem.* **2009**, 48, 7389-7393.
- [22] Umegaki, T., Yan, J.M., Zhang, X.B., Shioyama, H., Kuriyama, N., Xu, Q., *Int. J. Hydrogen Energy* **2009**, 34, 3816-3822.
- [23] Yan, J.M., Zhang, X.B., Han, S., Shioyama, H., Xu, Q., *J. Power Sources*, **2010**, 195, 1091-1094.
- [24] Yan, J.M., Zhang, X.B., Han, S., Shioyama, H., Xu, Q., *Angew. Chem. Int. Ed.* **2008**, 47, 2287-2289.
- [25] Özkar, S., *Appl. Surf. Sci.* **2009**, 256, 1272-1277.

- [26] Aiken III, J.D., Finke, R.G., *J. Mol. Catal. A: Chem.* **1999**, 145, 1-44.
- [27] Gubin, S.P., *Magnetic Nanoparticles*, Wiley-VCH Publishers, Weinheim, Germany, **2009**.
- [28] Finke, R. G., Özkar, S., *Coordination Chemistry Reviews*, **2004**, 248, 135-146.
- [29] Gubin, S.P., Kataeva, N.A., *Rus. J. of Coord. Chem.* **2005**, 32, 849-857.
- [30] International Energy Agency World Energy Outlook (WEO) **2009**, Paris, http://www.worldenergyoutlook.org/docs/WEO2009_es_english.pdf (last access date 20.07.2011).
- [31] Stephen, S., (Ed.), WWF The Energy Report: 100% Renewable Energy by **2050**.
http://assests.panda.org/downloads/101223_energy_report_final_print_2.pdf
(last access date 20.07.2011).
- [32] Thomas, C.D., et al, *Nature*, **2003**, 427, 145-148.
- [33] U.S. Department of Energy, *Hydrogen&Our Energy Future*, Energy Information Administration, Annual Energy Outlook **2005**, http://www1.eere.energy.gov/hydrogenandfuelcells/pdfs/hydrogenenergyfuture_web.pdf
- [34] US-DOE, *Energy Efficiency & Renewable Energy, Full Cell Technologies Program*,
http://www1.eere.energy.gov/hydrogenandfuelcells/pdfs/hydrogenenergyfuture_web.pdf
- [35] Sorensen, B., *Hydrogen and Fuel Cells: Emerging Technologies and Applications*, Elsevier Academic Press, San Diego, California, **2005**.
- [36] (a) Sandrock, G., Suda, S., Schlapbach, L., *Hydrogen in Intermetallic Compounds II, Topics in Applied Physics*, Springer, Verlag, Vol. 67, p 197, **1992**. (b) Sandrock, G., Yurum, Y., *Hydrogen Energy Systems: Production and Utilization of Hydrogen and Future Aspects*, NATO ASI Series, Kluwer Academic Publishers, **1994**.

- [37] Rosi, N.L., Eckert, J., Eddaoudi, M., Vodak, D.T., Kim, J., O'Keeffe, M., *Science*, **2003**, 300, 1127.
- [38] (a) Dillion, A.C., Jones, K.M., Bekkedahl, T.A., Kiang, C.H., Bethune, D.S., Heben, M., *Nature*, **1997**, 386, 377; (b) Park, C., Anderson, P.E., Chambers, A., Tan, C.D., Hidago, R., Rodriquez, N.M., *J. Phys. Chem. B*, **1999**, 103, 10572; (c) Liu, C., Fan, Y.Y., Liu, M., Wei, Y.L., Lu, M.Q., Cheng, H.M., *Science*, **1999**, 286, 1127; (d) Nikitin, A., Ogasawara, H., Mann, D., Denecke, R., Zhang, Z., Dai, H., Cho, K., Nilsson, A., *Phys. Rev. Lett.* **2005**, 95, 225507.
- [39] (a) Marrero-Alfonso, Y.E., Beard, A.M., Davis, T.A., Matthews, M.A., *Ind. Eng. Chem. Res.*, **2009**, 48, 3703; (b) Umegaki, T., Yan, J-M., Zhang, Z-B., Shioyama, H., Kuriyama, N., Xu, Q., *Int. J. Hydrogen Energy* **2009**, 34, 2303.
- [40] Demirci, Ü.B., Miele, P., *Energy Environ. Sci.* **2009**, 2, 627-637.
- [41] Amendola, S.C., Onnerud, P., Kelly, M.T., Petillo, P.J., Sharp-Goldman, S.L., Binder, M., *J. Power Sources*, **1999**, 84, 130.
- [42] Amendola, S.C., Sharp-Goldman, S.L., Janjua, M.S., Spencer, N.C., Kelly, M.T., Petillo, P.J., Binder, M., *Int. J. Hydrogen Energy*, **2000**, 25, 969.
- [43] (a) Demirci, Ü.B., Miele, P., *J. Power Sources*, **2007**, 172, 676. (b) Liu, B.H., Li, Z.P., *J. Power Sources*, **2008**, 187, 291. (c) Liu, Z.P. Li, *J. Power Sources*, **2008**, 187, 527.
- [44] (a) Schlesinger, H.I., Brown, H.C and Finholt, A.E., 711, 205 (1963). (b) S. W. Chaikin and W. G. Broftn, 71, 122 (1949); (c) A. Stewart, Master's Thesis, University of Chicago (1948).
- [45] (a) Amendola, S.C., Janjua, J.M., Spencer, N.C., Kelly, M.T., Petillo, P.J., Sharp-Goldman, S.L., Binder, M., *Int. J. Hydrogen Energy*, **2000**, 25, 969. (b) Lee, J.Y., Lee, H.H., Lee, J.H., Kim D.M., Kim J.H., *J. Electrochem. Soc.*, **2002**, 149(5), A 603.

- [46] U.S. Department of Energy. Independent review. November 2007. Golno-go recommendation for sodium Borohydride for on-board vehicular hydrogen storage. NREL/MP-150-42220.
- [47] Karkamkar, A., Aardahl, C., Autrey, T., *Materials Matters*, **2007**, 2, 2.
- [48] Klooster, W.T., Koetzle, T.F., Siegbahn, P.M., Richardson, T.B., Crabtree, R.H., *J. Am. Chem. Soc.*, **1999**, 121, 6337.
- [49] Richardson, T.B., de Gala, S., Crabtree, R.H., *J. Am. Chem. Soc.*, **1995**, 117, 12785.
- [50] Züttel, A., *Mater. Today*, **2003**, 6, 24.
- [51] (a) Baitalow, F., Baumann, J., Wolf, G.; Jaenicke, K., Leitner, G. *Thermochim. Acta*, **2002**, 391, 159-168; (b) Wolf, G., Baumann, J., Baitalow, F., Hoffman, F. P. *Thermochim. Acta*, **2000**, 343, 19-25.
- [52] Erdogan, H., Metin, Ö., Özkar, S. *Phys. Chem. Chem. Phys.* **2009**, 11, 10519-10525.
- [53] Xu, Q., Chandra, M. *J. Alloys Compd.* **2007**, 446-447, 729-732.
- [54] (a) Jaska, C. A., Temple, K., Lough, A. J., Manners, I. *Chem. Commun.* **2001**, 962-963. (b) Denney, M. C., Pons, V., Hebden, T. J., Heinekey, D. M., Goldberg, K. I. *J. Am. Chem. Soc.* **2006**, 128, 12048-12049.
- [55] (a) Xu, Q, Chandra, M., *J. Alloys Compd.* **2007**, 446-447, 729-732. (b) Jiang H.L., Singh, S.K., Yan, J.M, Zhang, X.B, Xu, Q., *ChemSusChem.* 2010, 3, 541-549. (c) Umegaki, T., Yan, J.M., Zhang, X.B., Shioyama, H., Kuriyama, N., Xu, Q., *Int. J. Hydrogen Energy*, **2009**, 34, 2303-2311. (d) Diwan, M., Hanna, D., Varma, A., *Int. J. Hydrogen Energy*, **2010**, 35, 577-584.
- [56] a) Simagina, V.I., Storozhenko, P.A., Netskina, O.V., Komova, O.V., Odegova, G.V., Larikhev, Y.V., Ischenko, A.V., Ozerova, A.M., *Catal. Today*, **2008**, 138, 253. b) Yan, J.M., Zhang, X.B., Han, S., Shiomaya, H., Xu, Q., *Angew. Chem., Int. Ed.*, **2008**, 47, 2287.
- [57] Xu, Q., Chandra, M., *J. Power Sources*, **2006**, 163, 364.
- [58] Aiken III J.D., Lin, Y., Finke R.G., *J. Mol. Catal. A*, **1996**, 114, 29.

- [59] (a) Schmid, G. (Ed), *Clusters and Colloids: From Theory to Applications*, VCH Publishers, New York, **1994**. (b) Jongh, L.J.(Ed), *Physics and Chemistry of Metal Cluster Compounds*, Kluwer Publishers, Dordrecht, **1994**.
- [60] Simon, U., Schön, G., Schmid, G., *Angew Chem. Int. Ed. Eng.*, **1990**, 248, 1186.
- [61] Glanz, J., *Science*, **1995**, 269, 1363.
- [62] Antonietti, M., Göltner, C., *Angew Chem. Int. Ed. Eng.*, **1997**, 36, 910.
- [63] Elghanian, R., Storhoff, J.J., Mucic, R.C.; Setinger, R.L., Mirkin, C.A., *Science*, **1997**, 277, 1078.
- [64] Colvin, V.L., Schlamp, M.C., Alivisatos, A.P., *Nature*, **1994**, 370, 354.
- [65] Sonti, S.V., Bose, A., *J. Colloid Int. Sci.*, **1995**, 170, 575.
- [66] Vossmeier, T., Delenno, E., Heath, J.R., *Angew. Chem., Int. Ed. Eng.*, **1997**, 36, 1080.
- [67] (a) Schmid, G., Maihack, V., Lantermann, F., Pechel, S., *J. Chem. Soc. Dalton Trans.*, **1996**, 199, 589. (b) Lin, Y., Finke, R. G., *J. Am. Chem. Soc.*, **1994**, 116, 8335. (c) Bönneman, H.; Braun, G.A., *Angew Chem. Int. Ed. Eng.*, **1996**, 35, 1992. (d) Lewis, L.N.; Lewis, N., *J. Am. Chem. Soc.*, **1986**, 108, 7228. (e) Wilcoxon, J.P.; Martinho, T.; Klavetter, E.; Sylwester, A.P., *Nanophase Mater.* **1994**, 771. (f) Na, Y.; Park, S.; Bong, S.H.; *J. Am. Chem. Soc.*, **2004**, 126, 250. (g) Pelzer, K.; Vidoni, O.; Phillot, K.; Chaudret, B.; Collière, V., *Adv. Func. Mater.*, **2003**, 12, 118. (h) Hostetler, M.; Wingate, J.; Zong, C.; Evans, N.; Murray, R., *Langmuir*, **1998**, 14, 17-30 (i) Pelzer, K.; Phillot, K.; Chaudret, B., *Z. Anorg. Allg. Chem.*, **2003**, 629, 1217.
- [68] Pool, R., *Science*, **1990**, 248, 1186
- [69] Borman, V.D., Borisjuk, P.V., Pushkin, M.A., Tronin, I.V., Tronin, V.N., *Cond-mat.mess-hall*, **2010**.
- [70] (a) Schmid, G., Bäumle, M., Geerkens, M., Heim, I., Osemann, C., Sawitowski, T., *Chem. Soc. Rev.*, **1999**, 128, 79. (b) Schmid, G., *Chem. Rev.*, **1992**, 92, 1709.

- [71] (a) Naves, P.M., Gonzaga, T.N., Monte, A.F.G. and Dantas, N.O. *J. Non-Crystal. Solids*, **2006**, 352, 3633–3635. (b) Tang, H., Xu, G., Weng, L., Pan, L. and Wang, L. **2004**, 52, 1489–1494. (c) Sashchiuk, A. and Lifshitz, E, *J. Sol-Gel Sci. Technol.* **2002**, 24(1), 31–38. (d) Patel, A.A., Wu, F., Zhang, J.Z., Torres-Martinez, C.L., Mehra, R.K., Yang, Y. and Risbud, S.H., *J. Phys. Chem.* **2000**, B 104, 11598–11605.
- [72] Campbell, T.C., *Science*, **2004**, 306, 234-235 and references therein
- [73] Verwey, E. J. W., Overbeek, J. T. G., *Theory of the Stability of Lyophobic Colloids*, Dover Publications: Mineola, New York, **1999**.
- [74] Ninham, B. W., *Adv. Coll. Int. Sci.*, **1999**, 83.
- [75] Özkar S., *Appl. Surf. Sci.*, **2009**, 256, 1272 and references therein.
- [76] Ott, L.S., Hornstein, B.J., Finke, R.G., *Langmuir*, **2006**, 22, 9357.
- [77] Hirai, H., Yakura, N., *Polym. Adv. Tech.* **2001**, 12, 174.
- [78] Hirai, H., Toshima N., *In Catalysis by Metal Complexes: Tailored Metal Catalyst*, Iwasawa Y (Ed.), Reidel Publishing Company, Dordrecht, **1986**.
- [79] Hirai, H., Toshima N., *In Catalysis by Metal Complexes: Tailored Metal Catalyst*, Iwasawa Y (Ed.), Reidel Publishing Company, Dordrecht, **1986**.
- [80] Toshima, N., *Macromol. Symp.*, **2000**, 156, 45.
- [81] Schmid, G., *Nanoparticles: From Theory To Application*, Wiley-VCH, Weinheim, **2004**.
- [82] Zahmakiran, M., Özkar, S., *Inorg. Chem.*, **2009**, 48, 8955
- [83] Shi, J., 06502/CISM/jys, Steric Stabilization, **2002**.
- [84] Feldheim, D. R., Foss Jr, C. A. (Eds.), *Metal Nanoparticles: Synthesis, Characterization, and Applications*, Marcel Dekker, New York, **2002**.
- [85] Willner, I., Mandler, D., *J. Am. Chem. Soc.*, **1989**, 111, 1330.
- [86] Rodriguez, J.A., Garcia, M.F., *Synthesis, Properties, and Applications of Oxide Nanomaterials*, WILEY, New Jersey, 2007
- [87] Bönneman, H., Richards, R. M., *Eur. J. Inorg. Chem.*, **2001**, 10, 2445
- [88] (a) Tano, T., Esumi, K., Meguro K., *J. Colloid Interface Sci.*, **1989**, 133, 530. (b) Esumi, K., Tano, T., Meguro, K., *Langmuir*, **1989**, 5, 268. (c) Dhas, N. A.,

- Suslick, K. S., *J. Am. Chem. Soc.*, **2005**, 127, 2368. (d) Suslick, K. A., Choe, S.-B., Cichowias, A. A., Grinstaff, M. W., *Nature*, **1991**, 353, 414.
- [89] Duteil, A., Queau, R., Chaudret, B., Mazel, R., Roucau, C., Bradley, J. S., *Chem. Mater.*, **1993**, 5, 341
- [90] Klabunde, K. J., Habdas, J., Cardenas-Trivino, G., *Chem. Mater.*, **1989**, 1, 481.
- [91] (a) Reetz, M. T., Helbig, W., Quaiser, S. A., *In Active Metals: Preparation, Characterization, Applications*, VCH: New York, **1996**. (b) Reetz, M. T., Helbig, W., *J. Am. Chem. Soc.*, **1994**, 116, 7401.
- [92] Ertl, G., Knözinger, H., Schtüh, F., Weitkamp, J., (Eds.), *Handbook of Heterogeneous Catalysis 2nd Edition, Volume 1*, Wiley-VCH, New York, **1990**.
- [93] Thomas, J. M., Thomas, W. J., *Principles and Practice of Heterogeneous Catalysis*, VCH, New-York, **1997**.
- [94] (a) Rothenberg, G. *Catalysis: Concepts and Green Applications*, Wiley-VCH, Weinheim, 2008. (b) Smith, G.V., Notheisz, F., *Heterogeneous Catalysis in Organic Chemistry*; Academic Press, San Diego, 1999.
- [95] G.F. Swiegers (Ed.), *Mechanical Catalysis: Methods of Enzymatic, Homogeneous and Heterogeneous Catalysis*, Wiley&Sons, New Jersey, **2008**.
- [96] http://users.humboldt.edu/rpasek/C107.F09/Chem_Discuss/ChemEquil_Ans.html (last access date 20.07.2011).
- [97] (a) Cheysaac, P., Kofman, R., Merli, P.G., Migliori, A., Stella, A. *Mater. Res. Soc. Symp. Proc.* **1994**, 332, 109. (b) Cheysaac, P., Kofman, R., Mattei, G., Merli, P. G., Migliori, A., Stella, A. *Superlattices Microstruct.* **1995**, 17, 47.
- [98] (a) Metin, Ö., Özkar, S. *Int. J. Hydrogen Energy*, **2007**, 32, 1707. (b) Metin, Ö., Özkar, S. *J. Mol. Catal. A: Chem.*, **2008**, 295, 39. (c) Metin, Ö., Özkar, S. *Energy&Fuels*, **2009**, 23, 3517. (d) Erdogan, H., Metin, Ö., Özkar, S. *Phys. Chem. Chem. Phys.*, **2009**, 11, 10519. (e) Metin, Ö., Sahin, S., Özkar, S. *Int. J. Hydrogen Energy*, **2009**, 34, 6304.
- [99] Creighton, J.A.; Eadon, D.G., *J. Chem. Soc. Faraday Trans.*, **1991**, 87, 3881.

- [100] Waseda, Y., Muramatsu, A., *Morphology Control of Materials and Nanoparticles*, Springer-Verlag, Berlin, Germany, **2004**.
- [101] Wechuysen, B.M., *In-situ spectroscopy of Catalysts*, American Scientific Publishers, CA, USA, **2004**.
- [102] Niemantsverdriet, J.W., *Spectroscopy in Catalysis: An Introduction*, Wiley-VCH, Weinheim, Germany, **2000**.
- [103] Aiken III J.D., Finke R.G., *J.Mol. Catal. A: Chem.*, **1999**, 145, 1- 44.
- [104] (a) Schmid, G., Baumle, M., Geerkens, M., Heim, I., Osemann, C., Sawitowski, T., *Chem. Soc. Rev.* **1999**, 28, 179; (b) Schmid, G., Chi, L.F., *Adv. Mater.* **1998**, 10, 515. (c) Finke, R.G., in: D.L. Feldheim, Foss, C.A., Jr. (Eds.), *Metal Nanoparticles: Synthesis, Characterization and Applications*, Marcel Dekker, Inc., New York, **2002**, pp. 17–54 (Chapter 2). (d) Turton, R., *The Quantum Dot: A Journey into the Future of Microelectronics*, Oxford University Press, New York, **1995**. (e) Haberland, H. (Ed.), *Clusters of Atoms and Molecules*, Springer-Verlag, New York, **1994**. (f) Schmid, G. (Ed.), *Clusters and Colloids; From Theory to Applications*, VCH Publishers, New York, **1994**. (g) de Jongh, L.J. (Ed.), *Physics and Chemistry of Metal Cluster Compounds*, Kluwer Publishers, Dordrecht, **1994**.
- [105] Schmid, G., *Endeavour*, **1990**, 14, 172.
- [106] (a) Van Den Berg, J. P., Lucien, J. P., Germaine, G., Thielemans, G. L. B., *Fuel Processing Technology*. **1993**, 35, 119. (b) Corma, A., Martínez, A., Martínez-Soria, V., *Journal of Catalysis*, **2001**, 200, 259. (c) Bönemann, G. A., Braun, G. A., *Angew. Chem. Int. Ed.*, **1996**, 35, 1992. (d) Lewis, L. N., Lewis, N., *J. Am. Chem. Soc.*, **1986**, 108, 7228–7231. (e) Schmidt, T. J., Noeske, M., Gasteiger, H.A., Behm, R. J., Britz, P., Brijoux, W., Bönemann, H., *Langmuir*, 13, **1997**, 2591. (f) Reetz, M.T., Quaiser, S.A., Merk, C., *Chem. Ber.*, **1996**, 129, 741. (g) Reetz, M. T., Breinbauer, R., Wanninger, K., *Tetra. Lett.*, **1996**, 37, 4499. (h) Reetz, M.T., Lohmer, G., *J. Chem. Soc. Chem. Comm.*, **1996**, 1921. (i) Reetz, M.T., Breinbauer, R., Wedemann, P., Binger, P., *Tetrahedron*, **1998**, 54, 1233.

- [107] Widegren, J.A., Aiken, J.D., Özkar, S., Finke, R.G., Chem. Mater. **2001**, 13, 312-324.
- [108] Zotov, A.V., Kotova, Z.Y., Geokhimiya, **1979**, 285-290.
- [109] Creighton, J.A., Eadon, D.G., J. Chem. Soc. Faraday Trans. **1991**, 87, 3881-3891.
- [110] Watzky, M.A., Finke, R.G., J. Am. Chem. Soc. **1997**, 119, 10382-10400.

APPENDIX A

The kinetic data for the hydrolysis of ammonia borane catalyzed by PEG stabilized iron(0) nanoclusters studied by monitoring the hydrogen evolution depending on polymer concentration, catalyst concentration, substrate concentration, and temperature.

Table A.3. Volume of hydrogen generated versus time for the hydrolysis of ammonia borane catalyzed by PEG stabilized iron(0) nanoclusters in different polymer concentrations.

Time (min)	[PEG]/[Fe]=1	[PEG]/[Fe]=2	[PEG]/[Fe]=3	[PEG]/[Fe]=4	[PEG]/[Fe]=5
0	0	0	0	0	0
60	45.5	45.6	36.4	27.3	27.3
120	81.9	86.6	68.6	54.6	54.6
180	113.8	123.0	96.6	81.9	81.9
240	140.0	154.9	124.0	107.4	104.6
300	163.0	183.0	146.8	127.4	122.8
360	183.9	206.9	156.8	145.6	141.0
420	201.0	226.9	175.0	161.8	154.6
480	216.6	246.0	190.0	177.5	168.2
540	232.0	267.0	205.0	189.2	180.0
600	245.0	267.0	218.0	203.0	191.0
660	256.0	267.0	228.0	211.5	202.0
720	267.0		238.0	221.0	210.0
780	267.0		245.0	229.0	217.0
840	267.0		252.0	236.6	224.0
900			259.0	243.8	230.0
960			267.0	249.8	236.0
1020			267.0	255.7	242.0
1080			267.0	261.0	247.0
1140				267.0	252.0
1200				267.0	257.0

Table A.4. Volume of hydrogen generated versus time for the hydrolysis of ammonia borane catalyzed by PEG stabilized iron(0) nanoclusters in different iron(III) chloride concentrations in the range of 5-25 mM.

$[H_3NBH_3]=200\text{ mM}, 25 \pm 0.5\text{ }^\circ\text{C}.$

5 mM		10 mM		15 mM		20 mM		25 mM	
Time (min)	VH ₂ (mL)	Time (min)	VH ₂ (mL)	Time (min)	VH ₂ (mL)	Time (min)	VH ₂ (mL)	Time (min)	VH ₂ (mL)
0	0.00	0	0.00	0	0.00	0	0.00	0	0.00
1	6.88	1	11.00	1	23.38	1	26.13	1	48.13
2	12.38	2	19.25	2	34.38	2	38.50	2	82.50
3	17.88	3	26.13	3	45.38	3	49.50	3	107.25
4	23.38	4	33.25	4	55.00	4	66.00	4	130.62
5	28.88	5	39.25	5	63.25	5	93.50	5	136.00
6	33.38	6	44.63	6	72.88	6	103.13	6	136.00
7	38.88	7	49.13	7	78.38	7	110.00	7	136.00
8	43.00	10	63.13	10	92.13	8	116.88		
9	48.13	15	75.88	15	108.63	9	122.38		
10	52.25	20	87.88	20	122.38	10	127.88		
15	62.00	25	97.75	25	130.63	15	135.50		
20	71.30	30	106.75	30	135.50	20	135.50		
25	80.50	35	113.20	35	135.50	25	135.50		
30	89.63	40	119.10	40	135.50	30	135.50		
35	97.50	45	124.20						
40	103.25	50	128.10						
45	110.00	55	132.10						
50	115.30	60	135.50						
55	119.70	65	135.50						
60	123.20	70	135.50						

Table A.5. Volume of hydrogen generated versus time for the hydrolysis of ammonia borane catalyzed by PEG stabilized iron(0) nanoclusters in different H₃NBH₃ concentrations in the range of 100-1500 mM.

[FeCl₃]= 25.0 mM, 25 ± 0.5 °C.

Time (min)	100 mM	200 mM	300 mM	400 mM	500 mM	750 mM	1000 mM	1500 mM
0	0	0	0	0	0	0	0	0
1	9.1	18.2	27.3	41.0	54.6	56.5	59.6	60.2
2	18.2	36.4	50.1	77.4	100.0	104.6	109.8	111.9
3	25.5	52.8	72.8	109.3	136.4	142.5	149.5	152.8
4	31.9	67.3	92.0	136.6	168.3	176.4	186.8	189.0
5	37.8	80.1	109.2	159.3	195.6	205.7	217.0	221.3
6	41.9	92.0	123.8	177.5	218.4	230.8	244.6	249.9
7	46.4	101.1	136.5	193.9	238.2	252.6	268.3	274.3
8	50.4	110.2	148.3	207.5	256.2	272.0	290.2	297.5
9	54.0	117.5	158.4	219.3	272.4	290.6	310.5	318.4
10	57.6	123.0	168.5	229.4	286.2	306.0	328.0	337.6
11	60.1	128.0	177.6	239.5	300.0	322.0	344.7	354.6
12	63.6	132.0	186.7	246.8	312.0	336.3	360.7	371.7
13	67.0	135.0	193.9	252.3	324.0	348.4	374.9	386.0
14	67.0	135.0	200.0	257.0	334.0	358.7	388.0	401.8
15	67.0	135.0	200.0	262.0	334.0	368.9	400.5	413.2
16			200.0	267.0	334.0	378.0	410.8	424.4
17				267.0		378.0	410.8	

Table A.6. Volume of hydrogen generated versus time for the hydrolysis of ammonia borane catalyzed by PEG stabilized iron(0) nanoclusters at different temperatures in the range of 15-35 °C.

[FeCl₃]= 25.0 mM, [H₃NBH₃]= 200 mM

Time (min)	15 °C	20 °C	25 °C	30 °C	35 °C
0	0	0	0	0	0
1	9.5	13.3	18.2	24.7	32.3
2	17.0	24.7	36.4	45.6	60.8
3	24.7	34.3	49.8	62.7	83.6
4	31.5	43.7	61.2	76.0	102.6
5	38.0	51.0	72.6	89.3	117.8
6	44.5	58.5	84.2	100.7	129.2
7	52.0	66.0	94.8	111.2	135.0
8	57.5	72.8	103.2	118.2	135.0
9	64.0	79.6	110.3	125.8	135.0
10	70.0	85.6	117.5	130.6	
11	75.5	91.0	123.6	135.0	
12	82.0	96.7	128.0	135.0	
13	87.0	102.2	133.0	135.0	
14	92.0	107.9	135.0		
15	96.5	112.8	135.0		
16	101.0	117.2	135.0		
17	105.5	121.6			
18	110.0	125.4			
19	113.8	128.4			
20	117.6	131.4			
21	121.4	135.0			
22	125.2	135.0			
23	129.0	135.0			
24	132.0				
25	135.0				
26	135.0				
27	135.0				